Plant Physiology Preview. Published on March 19, 2010, as DOI:10.1104/pp.110.154856

Running head:

Diurnal transcript profiling in developing barley caryopses

Corresponding author:

Elke Mangelsen

Swedish University of Agricultural Sciences

Department of Plant Biology and Forest Genetics

P. O. Box 7080

SE-750 07 Uppsala

Phone: +46 18 67 3239

Fax: +46 18 67 33 89

Email: elke.mangelsen@vbsg.slu.se

Journal research area:

Genome Analysis

Title:

Significance of light, sugar and amino acid supply for diurnal gene regulation in developing barley (*Hordeum vulgare*) caryopses

Elke Mangelsen[1]*, Dierk Wanke[2]*, Joachim Kilian[2], Eva Sundberg[1], Klaus Harter[2], Christer Jansson[3]

* These authors contributed equally to this work.

[1]Department of Plant Biology and Forest Genetics, The Swedish University of Agricultural Sciences (SLU), P.O. Box 7080, SE-750 07 Uppsala, Sweden

[2] Center of Plant Molecular Biology (ZMBP), University of Tuebingen, Auf der Morgenstelle 1, D-72076 Tübingen, Germany

[3] Lawrence Berkeley National Laboratory, Earth Sciences Division, 1 Cyclotron Rd., Berkeley, CA 94720, U.S.A.

Footnotes:

Financial source:

This work was supported by grants from the Swedish Research Council for Environment, Agricultural Sciences and Spatial Planning (Formas), Stiftelsen August T. Larsson Fond, the Deutsche Forschungsgemeinschaft (DFG) HA2146/11-1, and in part by U. S. Department of Energy Contract DE-AC02-05CH11231 with Lawrence Berkeley National Laboratory.

Corresponding author:

Elke Mangelsen

elke.mangelsen@vbsg.slu.se

Abstract

The caryopses of barley (*Hordeum vulgare*), as of all cereals, are complex sink organs optimized for starch accumulation and embryo development. Whilst their early to late development has been studied in great detail, processes underlying the caryopses' diurnal adaptation to changes in light, temperature and the fluctuations in phloem-supplied carbon and nitrogen have remained unknown. In an attempt to identify diurnally affected processes in developing caryopses at the early maturation phase, we monitored global changes of both, gene expression and metabolite levels.

We applied the 22K Barley1 GeneChip microarray and identified 2,091 differentially expressed (DE) genes that were assigned to six major diurnal expression clusters. Principal component analysis (PCA) and other global analyses demonstrated that the variability within the dataset relates to genes involved in circadian regulation, storage compound accumulation, embryo development, response to abiotic stress, and photosynthesis. The correlation of amino acid and sugar profiles with expression trajectories led to the identification of several hundred potentially metabolite-regulated DE genes.

A comparative analysis of our dataset and publicly available microarray data disclosed suborgan-specific expression of almost all diurnal DE genes, with more than 350 genes specifically expressed in the pericarp, endosperm, or embryo tissues.

Our data reveal a tight linkage between day-night cycles, changes in light and the supply of carbon and nitrogen. We present a model that suggests several phases of diurnal gene expression in developing barley caryopses, summarized as starvation & priming, energy collection & carbon fixation, light protection & chaperone activity, storage & growth, and embryo development.

Introduction

Metabolic processes in plants and most other organisms operate in concert with day-night cycles. This coordination is accomplished by diurnal oscillations in transcriptional and posttranscriptional activities integrated by light, temperature, carbon status, and circadian signaling (Usadel et al., 2008 and references therein). Through this arrangement, metabolic pathways in the cell can sense and anticipate environmental cues.

The plant body is generally divided into net carbon exporting tissues, like mature leaves, and net carbon importing tissues, such as the endosperm of developing seeds. These source and sink tissues alike can sense day-night cycles. For sink organs this sensing is partially mediated via diurnal fluctuations in metabolite availability, or circadian rhythms in the source. A prime example is sucrose export from photosynthetically active tissues to sink organs, which slows down at night when carbon export depends on mobilization of transitory starch (Geigenberger and Stitt, 2000). In addition, since leaves export not only sugars but also amino acids it follows that sink organs should experience shifts in nitrogen supply as well. This communication between source and sink has a major impact on cellular functions in both types of organs and is further integrated with hormonal, particularly abscisic acid (ABA), signaling (Gutierrez et al., 2007; Baguma et al., 2008). In addition, sink organs exhibit circadian or circadian-like rhythms in gene activities independently of the metabolic output from the source (Baguma et al., 2008).

The cereal seed, called caryopsis, is an economically important sink organ. It comprises the filial embryo and endosperm that are surrounded by a maternal seed coat, which consists of the photosynthetically active palea, lemma, and pericarp tissues. Palea and lemma form the outermost layer of caryopses and are involved in the seed's protection from light damage and pathogen attack (Abebe et al., 2004). The pericarp, which is vital until late stages of caryopsis development, contains the vascular tissues and acts as central tissue for phloem unloading into the caryopsis (Patrick and Offler, 2001). The filial endosperm, which constitutes the largest part of the caryopsis during middle to late stages of development, accumulates storage starch

and nourishes the embryo during seed germination. In addition to these compartments, thin layers of specialized cells that connect the different sub-organs and/or function in transporting metabolites from vascular tissues into filial tissues, add to the complexity of the caryopsis (Patrick and Offler, 2001; Weschke et al., 2003; Abebe et al., 2004; Thiel et al., 2008; Sabelli and Larkins, 2009).

Metabolic and regulatory changes throughout the development of the barley (*Hordeum vulgare*) caryopsis, from early flowering to late seed maturation and germination processes, have been studied to a great extent (Sreenivasulu et al., 2006; Sreenivasulu et al., 2008; Radchuk et al., 2009). However, little is known about diurnal adaptations in the cereal caryopses and several aspects pose intriguing questions regarding the regulation of these processes.

To obtain a comprehensive understanding of the interplay between major metabolic processes in the caryopsis, like phloem unloading, embryo development, storage starch biosynthesis, photosynthate production, and turnover of transient starch in the green tissues, we set out to follow the transcriptional activities during a 24-h light-dark regime in intact barley caryopses. We used the 22K Barley1 GeneChip array (Close et al., 2004) and monitored levels of transcripts at different time points. A total of 2,091 differentially expressed (DE) genes were clustered into co-expressed and functional groups. To correlate oscillations in gene expression with metabolic activities, we measured metabolite levels for sugars and amino acids and found several hundred genes that are potential targets for metabolite-dependent gene regulation. A comparison of our DE genes and publicly available microarray data (Sreenivasulu et al., 2008) disclosed that the pericarp, endosperm and embryo contributed equally to the observed day-night diversity. Whilst the majority of diurnal DE genes were expressed in all suborgans tested, about 350 diurnal DE genes were assigned to specific parts of the caryopsis.

Results

Diurnal expression profiling of developing barley caryopses

We used barley caryopses at 11 to 12 days post anthesis (d.p.a.) to study diurnal changes in gene expression. This developmental stage, also referred to as early maturation phase, is characterized by high sucrose levels and a rapid accumulation of storage starch in filial tissues of the caryopsis (Borisjuk et al., 2004; Sabelli and Larkins, 2009). Caryopses from the mid region of the spike (Figure 1A and 1B) were sampled at six time points during the day. The first sample was harvested at 11d.p.a. one hour (1h) after the onset of darkness. The following day (12d.p.a.), samples were taken half an hour before and after the shift from dark to light phase (9h and 10h), at two time points in the middle of the light phase (17h and 20h), and one hour before the end of the light phase (23h after the onset of darkness). Using pooled plant material, we obtained highly reproducible data for two replicates at each time point. Correlation coefficients for the replicates ranged from 0.968 to 0.989 (data not shown). In total, 17,416 probesets (hereafter referred to as genes) were scored present and used for further data analysis (Table S1). For data verification, quantitative polymerase chain reaction (qPCR) experiments were performed for a subset of genes and revealed similar expression patterns (Figure S1).

Cluster analysis of genes showing diurnal expression patterns

To examine expressional changes in more detail, we calculated the total number of DE genes. On the basis of the 17,416 expressed genes a total of 2,091 (11%) DE genes could be assigned with significance (Figure 1C; Table S2). Subsequently, the expression trajectories of all 2,091 DE genes were subjected to k-means clustering and six main clusters (Set 1 to 6) were chosen, with each of them exhibiting a distinct minimum and maximum of expression (Figure 2A and Table S3). Set 1 (429 genes) can generally be described by an increase of expression during the night and a constant decrease of expression during the light phase. Interestingly, the expression trajectories of cluster Set 3 (518 genes) are complementary to Set 1 with a steady increase of transcript levels during the light phase and a decrease during the dark. Together, these two inversely correlated clusters represent about 45% of all DE genes. A remarkable feature of both clusters is that the major up- or downregulation of gene expression occurs in anticipation of the dawn, i.e. before the actual onset of light.

Genes clustered in Set 6 (223 genes) are characterized by a rapid induction upon transition from darkness to light at the onset of day and their expression is significantly reduced after the middle of the day. In contrast, the genes contained in Set 4 (241 genes) exhibit a rapid reduction of gene expression at the shift from darkness to light and a maximum of gene expression at the onset of the night. Genes of Set 2 (365 genes) can be described by rather high and stable transcript levels during the night and a constant reduction during the day. It is noteworthy that Set 3 transcript levels are restored during the last three hours of the light phase before the onset of the night. The genes contained in Set 5 (315 genes) are characterized by a maximum expression in the middle of the day followed by a decrease in transcript abundance during the later light phase and stable expression during the night.

We next performed an unbiased approach to estimate the contribution of the DE genes to the total variability observed within the experiment and subjected the dataset to Principal Component Analysis (PCA). We assumed that the genes contained in the six sets derived by the k-means clustering should make a distinct contribution to the entire variability of the dataset, which in turn would constitute an independent validation of the number of inferred gene clusters. Indeed, most DE genes overlapped with Principal Components PC1 to PC3 and contributed to more than 90 % of the expression variability observed in our dataset (Table S4). In addition, the six clusters mark three pairs of antagonistic Sets to be either highly correlated or anti-correlated to PC1, PC2 and PC3, which is supportive of our clustering procedure. Supplementary Table S4 lists those genes that exhibit high positive or negative correlation coefficients for the antagonistic pairs Sets 3 and 1 (for PC1), Sets 6 and 4 (for PC2) as well as Sets 5 and 2 (for PC3).

Functional annotations of the expression clusters using Gene Ontology

To determine whether the expression profiles in the six clusters correlated with functional activities they were classified into functional groups using the gene ontology (GO) terms. We caution that GO annotations could only be made for those probesets on the microarray that had been assigned in putative orthology to Arabidopsis based on their HarvEST annotation (Close et al., 2007). This was the case for about 70% of all probesets

(Table S1). In addition, we did not compute the error from different probesets that share the identical Arabidopsis gene as a best match in the HarvEST annotation. Hence, these genes contribute only once to the GO annotation and may thus add a bias to the analysis.

Ontologies for 'Biological Process', 'Cellular Component' and 'Molecular Function' are shown in Figures 2B and S3. For the individual six clusters, all exhibit a characteristic distribution of the GO categories. For example, genes related to nucleic acid binding ($p \leq 10^{-5}$) and transcription factor activities ($p \leq 0.001$) are overrepresented in Set 1 whereas they are underrepresented in the antagonistic Set 3 ($p \leq 0.01$; Figure 2A). Particularly, the presence of transcription-related genes in Set 1 is in line with the idea of the plants' strategy to anticipate the dawn. Further, we note that there is an overrepresentation of DE genes in the GO groups for stress responses ($p \leq 10^{-8}$). A closer look at the genes grouped in the stress-related categories revealed that a common stimulus for most of these genes was temperature stress. This was particularly true for genes in Sets 3 and 5 ($p \leq 10^{-4}$), which depict maximum transcript levels during the light phase. Another finding was that the GO categories 'extracellular' are dominated by Set 4 genes ($p \leq 0.01$) and may thus indicate that biosynthesis processes in the cell wall or transport predominantly occur during the later light and early dark phase. Notably, genes with 'nucleotide binding' ($p \leq 0.001$) capabilities are significantly depleted in Set 6, which translates into a lower necessity for ATP-dependent processes, like energized transport over membranes.

MapMan analysis of present genes

To aid visualization, the dataset was processed with the MapMan software (Thimm et al., 2004) that has recently been adapted to the Barley1 microarray (Sreenivasulu et al., 2008). Out of the 17,416 genes scored as present, there are 833 genes (5%) with a diurnal amplitude exceeding $\log_2 = 1$ (Table S1). As indicated in the MapMan screenshot shown in Figure 3, many genes involved in photosynthesis, carbohydrate metabolism and secondary metabolism undergo strong diurnal fluctuations. A Wilcoxon rank test ($p<0.05$) was performed to list those functional categories, so-called BINs, which showed an overrepresentation of highly fluctuating genes. As a result, BINs for genes involved in the response to abiotic stress, particular heat stress, and BINs related to photosynthesis

were among the most fluctuating ones (Table S5), thus being consistent with the overrepresentation of GO categories for abiotic stress and plastid-localization among the DE genes (Figures 2B and S4). A strong adaptation of metabolic processes in caryopses to the availability of incoming carbon and nitrogen sources is indicated by significant fluctuations of BINs for metabolism of proteins, amino acids and major carbohydrates (CHO). Significant fluctuations in BINs for biosynthesis of abscisic acid (ABA) and BINs summarizing ABA-responding genes such as late embryo abundant (LEA) and hordein genes, demonstrate the diurnal importance of ABA-regulated processes.

Diurnal fluctuations of sugar and amino acid levels in developing barley caryopses

In leaf tissues, transitory starch is accumulated during the light phase and degraded during the night for respiration and in order to support cell viability of both source and sink tissues. Complex regulatory and metabolic networks exist that enable the accurate partitioning of the carbon sources in the plant during the day (Lu et al., 2005; Smith et al., 2005; Zeeman et al., 2007). Nevertheless, the daily shift from carbon assimilation during the light phase to starch degradation at night results in substantial variations in leaf sugar levels during the day (Smith and Stitt, 2007). We wondered whether similar fluctuations of sugar contents occur in the cereal caryopsis, or whether the supply from the breakdown of transitory starch in source tissues would result in the maintenance of steady state sugar levels in the caryopsis. As is displayed in Figure 4A and Table S6, barley caryopses underwent significant fluctuations in sugar contents during the light and dark phases, with sucrose showing the biggest diurnal shifts in amplitude. The sugar levels were generally rather constant during the middle and end of the day, and then declined during the night. The pools for sucrose, glucose and ribose were almost depleted at the end of the dark phase. Just half an hour into the light phase, the amounts of ribose, glucose, fructose and kestose were restored to levels similar to those at the end of the photosynthetic active light phase. This indicates that as little as 30 minutes of light are enough to refill the supply of these sugars in the caryopsis. In contrast, refilling of the sucrose pool advanced considerably more slowly. After 30 minutes of light induction the sucrose levels were still roughly ten times lower than at the end of the previous day. The cycling pattern for sucrose suggests a rapid turnover in the caryopsis during the early

phase of the light period (Figure 4, Table S6), which can be explained by sucrose being the main carbon supply for the endosperm. However, in the middle of the day, sucrose levels are restored and sucrose accumulates until the end of the day. This, in turn, may reflect the saturation of sucrose-demanding pathways and a consistent supply of photosynthate during the later light phase. Levels of kestose, the primary product of fructan biosynthesis, showed a slight but steady increase during the day, which is consistent with the function of fructans in the photosynthetic partitioning process (Nagaraj et al., 2004).

Compared to the investigated sugars, changes in amino acid contents were less pronounced (Figures 4B to D and Table S6). A number of amino acids had constant levels during the night or showed minimum levels in the middle or end of the light phase. However, glutamine and glutamic acid are known to constitute the dominating transport forms of amino acids throughout the light phase of the day (Lam et al., 1995) and accordingly, their contents exhibited significant fluctuations. Moreover, we noted a generally high variability even between the pooled individuals for glutamine that was especially pronounced in the early morning samples.

In agreement with previous reports, we found elevated amounts of asparagine, which serves as an important nitrogen storage and transport compound for the allocation of nitrogen resources between source and sink organs, at the beginning of the night (Lam et al., 1995; Lam et al., 2003).

The levels of alanine, which serves as a precursor for several other amino acids, appeared to be tightly coupled to sucrose levels (correlation coefficient +0.68) and thus to carbohydrate metabolism (Figure 4 A and B). The correlation between sucrose and alanine levels is probably explained by their connection through glycolysis with the alpha-keto acid pyruvate, which is converted to alanine by a transamination (Pratelli and Pilot, 2007). Similar accumulation patterns were displayed for amino acids produced from the same or intersecting pathways. This was particularly evident for alanine, valine and serine as one group and, to a lesser extent, histidine, phenylalanine, tyrosine, as another. The amounts of glycine were notably lower than expected, which might be explained by the generally lower levels of photorespiration in Poaceae (Engel et al.,

2007; Perez-Lopez et al., 2009).

Correlation of gene expression and metabolite levels

To address the question whether metabolite levels are related to gene expression, we calculated the correlation coefficients of metabolite profiles and the trajectories of all expressed genes (Figures 5 and 6, Table S7). Using a minimum correlation coefficient of 0.8 as threshold to correlate the levels of amino acids and sugars to gene expression profiles, we found 877 positively and 878 negatively correlated gene expression trajectories (Table S7). The total number of genes in the cereal caryopsis that responded to sugars is likely underestimated because the correlation study of gene expression and metabolite levels was conducted on the DE genes only.

The amino acids glutamine, glutamic acid, asparagine and aspartic acid were linked with large numbers of correlating and anti-correlating genes. As these amino acids are known as the major transport forms of nitrogen in the phloem (Lam et al., 1995), this suggests an impact of incoming metabolites on gene expression in the caryopsis. As expected by their connected pathways, a large overlap of 47 correlated and 54 anti-correlated genes existed for sucrose and alanine. The high number of genes showing a positive correlation to proline, which acts as a compatible solute, further indicates a connection between diurnal gene regulation and adaptation to changes in osmotic conditions (Ashraf and Foolad, 2006).

Among the investigated sugars, sucrose had by far the highest linkage number of correlated and anti-correlated transcript profiles (352 and 434, respectively). Among the positively correlating genes we found those that have been shown to be sucrose responsive in other contexts or species. These were, for example, the gene for granule bound starch synthase1b *HvGBSS1b* (Contig12208_at) and for the sucrose:fructan 6-fructosyltransferase *Hv6-SFT* (Contig3392_at) (Dian et al., 2003; Nagaraj et al., 2004). Also, expression of a trehalose-6-phosphate phosphatase-like gene *TPP-like* (HS16E24u_s_at) appeared to follow the sucrose levels, suggesting its potential role in sugar-signaling (Gomez et al., 2005). Several genes putatively involved in the

biosynthesis of the cell wall, such as a callose synthase-like gene (Contig19065_at) and two arabinofuranosidase-like genes (Contig5239_at, S0001000058H07F1_s_at), were also found among the positively correlated genes (Table S7). A dozen genes related to photosynthesis were found to be negatively correlated to sucrose, as expected by the inhibitory effect of sucrose on photosynthetic processes (Koch, 1996; Paul and Pellny, 2003). The negative correlation for the beta-amylase gene *HvBAM5* (Contig11522_at) is indicative of starch degradation occurring in times of sucrose starvation (Smith et al., 2005). For a more global investigation, a GO classification of genes with an expression profile that correlated to sucrose levels was performed (Figure S4). As a result, genes of the GO categories 'developmental processes' and 'cell organization and biogenesis' had a greater tendency to positively correlate to sucrose levels in the caryopsis, whereas genes negatively correlated to sucrose levels were more often related to the GO terms 'transcription' and 'transport'.

Expression profiles for genes involved in sucrose and starch metabolism

As we expected sucrose and starch metabolism to be affected by diurnal changes, we screened the Barley1 GeneChip for unambiguous probesets that represent genes involved in these processes. In order to assign genes to a given probeset, the Barley1 GeneChip was annotated using the HarvEST software version 1.73 (Close et al., 2007). Moreover, probesets representing previously described isoforms of genes involved in carbohydrate metabolism in barley were annotated manually to reduce the risk of false annotations. Out of 70 genes with a documented or potential role in sucrose, starch and fructan metabolism and regulation, 58 genes were represented on the microarray and 23 genes were DE in our experiment. Table 1 provides their common gene names, corresponding probesets and diurnal $\log_2$-amplitudes, as well as the expression cluster group for DE genes. The precise expression trajectories of the genes are shown in Figure 7.

Contained within the 2,091 DE genes, we identified several of the key genes involved in sucrose transport and metabolism, such as the cell wall invertase gene 1 *HvCWINV1*, and genes for a sucrose transporter *HvSUT2*, hexose transporter *HvHSTP1* and sucrose:fructan 6-fructosyltransferase *Hv6-SFT*. For genes related to starch metabolism, those encoding the large subunit of AGPase (*HvAPL1*), Granule bound starch synthase 1b

(*HvGBSS1b*), Starch Branching Enzyme 2b (*HvSBEIIb*), Limit Dextrinase (*HvLD*), Glucan, water dikinase 1 (*HvGWD1*), Isoamylase 3 (*HvISA3*) and beta-amylase 5 (*HvBAM5*) were among the DE genes. In addition, the Fructan 1-exohydrolase gene (*Hv1-FEH*), probably involved in fructan biosynthesis and degradation (Van Den Ende et al., 2003; Lothier et al., 2007), underwent strong diurnal fluctuation in expression. However, there were no pronounced diurnal variations in transcript levels for many of the genes responsible for metabolic or regulatory steps in starch biosynthesis, such as genes for Sucrose Synthases 1 and 2 (*HvSuSy1* and *HvSuSy2*), Isoamylases 1 and 2 (*HvISA1* and *HvISA2*), Starch synthases 1 and 2 (*HvSs1* and *HvSs2*) and SUSIBA2 (*HvWRKY46*). Next to genes with a known function in the conversion from sucrose to starch, we found several candidate genes potentially involved in sucrose signaling to be DE, such as genes for a hexokinase (*HvHXK1*), two trehalose-phosphate metabolic enzymes (*TPS-like* and *TPP-like*), and the WRKY transcription factor gene *HvWRKY41* (Rolland et al., 2006). We also noted that several genes of the ferredoxin/thioredoxin system underwent diurnal regulation. These were a Ferredoxin-NADP reductase gene and four putative thioredoxin (*Trx*) genes, among them the amyloplast-located *Trx m*. Several of the 43 identified Trx *m* targets in wheat amyloplasts (Balmer et al., 2006) were found to be DE in our study, among them the ADP-glucose transporter gene *HvNST1* and the gene for the large subunit of the ADP-glucose phosphorylase *HvAPL1*.

Combined microarray analysis of spatial gene expression patterns

To gain a more global overview of the spatial distribution of diurnal changes in gene expression, we combined our dataset with previously published microarray data that investigate the changes in gene expression in endosperm, embryo and pericarp tissues during caryopsis development (Sreenivasulu et al., 2008). Rather than looking at the developmental expression profiles of the three suborgans separately, we intended to identify those genes that were either commonly expressed in all suborgans or specific to a single suborgan. As shown in Figure 8A and Table S8, we found 3,093, 1,977 and 289 genes to be specifically expressed in pericarp, endosperm and embryo tissues, respectively. Hence, about one third of all present genes in the study of Sreenivasulu et al. (2008) had a suborgan-specific spatial expression pattern. In addition, all three

suborgans investigated contributed equally to the set of diurnally expressed genes identified in our study, with 11% of pericarp and endosperm genes (1600 and 1776 genes, respectively) and 10% of the embryo genes (1503 genes) exhibiting significant day-night fluctuations (Figure 8A and Table S8). Nevertheless, the majority of DE genes were not tissue-specific, but expressed in two or three of the suborgans tested. The overlap of tissue-specific and diurnally regulated genes was relatively low, indicating that only 7% (202 genes) of pericarp-specific, 8% (159 genes) of endosperm-specific and 5% (14 genes) of embryo-specific genes underwent diurnal fluctuations (Figure 8B and Table S8). Only 224 diurnal DE genes were not detected in the dataset of Sreenivasulu et al. (2008), suggesting that they were either expressed below detection levels in the sampled developmental stages or that they belong to a group of palea/lemma-specific genes that have not been probed. In summary, the combined analysis suggests that the majority of diurnally regulated genes have a function in several of the caryopsis tissues. On the other hand, many tissue-specific genes were identified among those that were diurnally regulated, prompting a speculation about tissue-specific pathways for diurnal regulation.

Quantification of spatial gene expression

In order to verify the suborgan presence predicted by the comparative microarray analysis described above, we applied quantitative real time PCR (qPCR) to investigate the spatial expression of a number of gene candidates. As shown in Figure 9, the selected genes showed distinct spatial expression patterns in endosperm, pericarp, husk and embryo tissues. In accordance with their role in mobilization of transitory starch (Smith et al., 2005), *HvBAM5*, *HvGWD1*, and *HvISA3* were predominantly expressed in the photosynthetically active pericarp tissues. A potential role of Plant Glycogenin-like Starch Initiation Proteins (PGSIP) in starch biosynthesis has previously been suggested by Chatterjee et al. (2004). An orthologous gene, *HvPGSIP2*, which was found to be DE during the day (Table 1), was mainly expressed in green tissues of the caryopsis. In contrast, its paralog *HvPGSIP1* that showed an expression profile negatively correlated to sucrose levels of the caryopsis (Table S7) was mainly expressed in endosperm tissue.

High expression levels in endosperm tissues were also found for the genes encoding

SUSIBA2 (*HvWRKY46*) and Limit Dextrinase (*HvLD*), confirming earlier findings (Burton et al., 1999; Sun et al., 2003). The diurnally fluctuating transcripts for *HvWRKY41* (Mangelsen et al., 2008) could mainly be detected in endosperm and pericarp tissues. As was previously observed for the Isoamylase 1 gene (*HvISA1*) (Sun et al., 1999), the Isoamylase 2 gene in barley (*HvISA2*) was preferentially expressed in the endosperm, whereas *HvISA3* transcripts were located in the pericarp.

Discussion

Photocycles, thermocycles, and the circadian clock together phase cellular activities in plants to generate diurnal oscillations in gene expression, metabolism and physiology (Wijnen and Young, 2006; Michael et al., 2008). We expected that relatively few DE genes in a sink organ such as the cereal caryopsis should be responsive to light signals, as only genes in the pericarp and the husk would be directly influenced by photocycles. Thus, we assumed that in the barley caryopsis, a major portion in diurnal oscillations of gene expression is conveyed through fluctuations in metabolite availability.

To gain an insight into these presumed relationships, we analyzed day-night cycles in gene expression and monitored the metabolite accumulation alongside, which subsequently allowed the correlation of metabolite availability and its putative effects on gene expression in barley caryopses. However, we are aware that observed transcript levels do not necessarily reflect protein levels or protein activity, and thus, our conclusions on gene function and interactions must be considered as tentative.

Diurnal regulation of starch metabolism and sugar signaling

Nearly all steps in the conversion from sucrose to starch or fructan have the potential to be diurnally regulated (Table 1 and Figure 7). The majority of genes involved in these processes were expressed in all suborgans of the caryopsis and, hence, are of general importance in various cell types (Table S8). The combined analysis with the dataset of Sreenivasulu et al. (2008) revealed only a few genes that were unambiguously located to the pericarp and endosperm, respectively (Table 1). However, the comparison with recent published studies on the spatial distribution of barley transcripts (Radchuk et al., 2009) and sub-organ localization using qPCR (Figure 8) allowed us to identify the predominant

location of several of these genes and to shed light on several diurnal regulatory aspects occurring in the developing caryopsis.

Of the genes encoding enzymes involved in starch elongation, branching and trimming (Smith, 1999, 2001; Smith et al., 2005; Hannah and James, 2008), *HvLD*, *HvISA3*, as well as the genes for starch branching enzyme IIb (*HvSBEIIb)* and starch synthase IIIb (*HvSSIIIb*) displayed diurnal regulation (Table 1 and Figure 7). As reported earlier (Sun et al., 1998; Burton et al., 1999; Radchuk et al., 2009), the transcripts of *HvSBEIIb* and *HvLD* were mainly found in the endosperm and are thus likely to be involved in the biosynthesis of storage starch (Table 1 and Figure 8). The expression of these genes peaked during the middle to late light phase, when sugar supply was at its maximum. The *HvSSIIIb* gene (Radchuk et al., 2009), which is preferentially expressed in the endosperm, was strongly induced in anticipation of the light rather than being correlated to high sugar levels (Figure 2 and Figure 7). Hence, its transcript levels peaked prior to those of *HvLD* and *HvSBEIIb* (Figure 7).

Furthermore, our data suggests an involvement *of HvISA3* in the production of transient starch, especially in the pericarp, during the light phase (Figures 7, 8 and 10). A similar function was recently demonstrated for isoamylase paralogs in Arabidopsis (Streb et al., 2008). The specific roles of *HvISA1* and *HvISA2* remain unclear (Burton et al., 2002) and neither seem to be under diurnal control (Table 1). However, the high expression levels of *HvISA2* in the endosperm suggest a prominent role during storage starch synthesis (Figure 8).

Not only biosynthesis but also the degradation of starch follows a diurnal pattern. We found the expression of *HvGWD1* and *HvBAM5*, both with a predicted role in starch degradation (Smith et al., 2005; Smith and Stitt, 2007; Zeeman et al., 2007) to be diurnally regulated. Expression of *HvGWD1* peaks at the onset of night and, thus, prior to *HvBAM5* (Figure 7), which is in line with the idea that phosphorylation by GWD1 prepares insoluble glucans for degradation by beta-amylases (Hejazi et al., 2008). The *HvBAM5* gene, encoding a presumed plastidial enzyme, exhibited high expression levels in the pericarp with a profile that was negatively correlated to sucrose content (Figure 9, Table S7). This observation lends support to a role of HvBAM5 in the degradation of

transitory starch during the night with granular starch and/or linear maltodextrins as substrate (Fulton et al., 2008; Radchuk et al., 2009). Moreover, activation of *HvBAM5* by sucrose starvation at the end of the night contrasted to the activity of genes involved in the initial metabolism of sucrose, such as *HvCWINV1*, *HvSUT2*, and *HvSTP1* (Figure 7).

Little is known about HXK function in barley despite its enrollment in sugar signaling and targeting of carbon into downstream metabolic pathways (Rolland et al., 2006). Although at least seven *HvHXK* genes are encoded in the barley genome, only *HvHXK1* followed a distinct diurnal expression profile with high transcript levels at night (Set 2; Figure 7). Interestingly, *HvHXK1* and *HvHXK2* transcripts showed exclusive expression in pericarp tissues (Table 1 and Table S8).

Sugar signaling networks may cause diurnal regulation of a large subset of genes in the barley caryopsis

A total number of 882 DE gene expression profiles exhibited positive or negative correlation to sugar levels (Figure 5 and Table S7). Hence, a significant fraction of those genes might act downstream of, or participate in, a sugar dependent signaling cascade. In Arabidopsis seedlings more than 4,000 diurnally fluctuating genes are affected by changing sucrose levels and many of the rapidly sucrose-induced or -repressed genes correlate either positively or negatively to diurnal sucrose levels (Blasing et al., 2005; Osuna et al., 2007).

As expected, positive correlation to sucrose was found for genes encoding enzymes in the starch biosynthetic pathway (Table S7) and for genes involved in sucrose transport. The sucrose transporter *HvSUT1* is thought to play a central role in the determination of endospermal sucrose levels, while the role of its paralog *HvSUT2*, which is expressed in all parts of the caryopsis, is yet unknown (Weschke et al., 2000; Endler et al., 2006; Thiel et al., 2008). Expression of *HvSUT2* peaked when sucrose levels were at a maximum and expression levels of *HvSUT1* were at a transient minimum. Thus we speculate that in times of excess sucrose, HvSUT2 facilitates a redirection of the sucrose flux into suborgans other than the endosperm (Figure 7). Co-expression of *HvSUT2* and the

fructan biosynthesis genes *Hv6-SFT* and *Hv1-FEH* suggests a concerted role for an intermediate carbon storage in vacuoles to provide sink strength of the caryopsis (Vijn and Smeekens, 1999). The positive correlation of *Hv6-SFT* and *Hv1-FEH* and sucrose further indicates that these genes are sucrose inducible also in sink organs, as previously described for leaves (Nagaraj et al., 2005). Finally, more than 240 genes were found to correlate to kestose levels and several of these genes are likely to be involved in fructan metabolism.

We notice that several genes with negative correlation to sucrose encode photosynthesis-related proteins, which highlights the inhibitory effect of sucrose on photosynthesis (Pego et al., 2000). Other negatively correlated genes are glycosyl hydrolases with ß-glucosidase activities, and glycosyl hydrolases that presumably act on mannose and xylose (Table S7). This implies hemicellulose degradation at low sucrose levels and supports the idea of hemicellulose and cellulose mobilization to supply energy under sucrose-limiting conditions (Contento et al., 2004; Hoch, 2007; Lee et al., 2007). Anti-correlation of profiles for several transcription factors and kinase genes with sucrose levels support the idea that the absence of sucrose as the main energy-providing carbon molecule rather than its presence has an impact on cellular signaling (Blasing et al., 2005).

Nitrogen signaling may regulate gene expression in developing caryopses of barley

In accordance with the pronounced diurnal fluctuations of the major transport forms of amino acids, glutamine, glutamic acid, asparagine and aspartic acid, we identified several genes related to their metabolism to undergo strong diurnal fluctuations (Tables S2 and S5). Whether this hints at a dual function of these amino acids, as both substrates for protein biosynthesis and signaling molecules, is unclear and needs to be addressed by further investigation as, generally, most of the predicted nitrogen and carbon/nitrogen (C/N) signaling matrices in plants are still far from being resolved (Lam et al., 1995; Coruzzi and Zhou, 2001; Zheng, 2009). Nevertheless, we found five genes for amino acid permeases (AAPs) to be diurnally regulated, out of which three showed a strong correlation to glutamine and glutamate levels (Tables S2 and S7). The diurnal and spatial

expression profiles of AAP genes are diverse and further studies are required to unravel their potential role in the control of amino acid levels in the developing seeds, as recently described for orthologous AAPs in Arabidopsis and pea (Weigelt et al., 2008; Sanders et al., 2009). In addition to amino acids, phloem-derived peptides contribute significantly to the N-status and regulate development in developing seeds (Miranda et al., 2003; Li et al., 2009). The diurnal expression of eleven peptide transporter genes (PTR) points at a tight diurnal control of the N-status in seeds via peptide import (Table S3). Finally, the observed positive correlation of a potential ortholog to *TIMING OF CAB EXPRESSION 1* (*TOC1*) (Contig11872_at) and glutamate (Table S7) raises the question whether there is a link between nitrogen and circadian signaling in barley caryopses, as previously postulated for Arabidopsis leaves (Gutierrez et al., 2008).

Embryo development genes undergo diurnal regulation

A noteworthy feature of the list of DE genes (Table S1) is the over-representation of genes potentially crucial to embryo development, such as putative orthologs to so-called embryo defective (EMB) and maternal effect embryo arrest (MEE) genes from Arabidopsis (Tzafrir et al., 2004). Indeed, a minimum of 21 genes, which could be linked to embryo development via their annotations, were found to exhibit diurnal expression patterns. Whilst all MEE-like DE genes found have unknown functions, the protein products of several EMB-like DE genes have enzymatic activities in nucleotide and amino acid biosynthesis. Others are described as constituents of the nuclear pore and the proteasome complex, underlining their pivotal cellular roles. Interestingly, the majority of embryo developmental genes fall into Sets 3 and 2 with eight and four genes, respectively (Table S3). This suggests that processes vital for embryo development are mainly activated during the late light period or at night (expression peak of Sets 3 and 2, respectively). In line with this notion, only two embryo development-related genes are found in Set 6 and none in Set 5; clusters characterized by low expression levels at late day and night times.

Additionally, a minimum of 11 LEA genes were diurnally expressed. Strikingly, seven LEA genes cluster into Set 6 whereas the other clusters contain only one or even not a

single LEA gene (Table S3). The trajectories of Set 6 genes suggest that LEA gene expression and, hence, accumulation of storage proteins preferably occurs at times of maximum photosynthate supply, starting immediately after the onset of light. In addition, one of the long-term functions of LEA proteins is the induced desiccation tolerance of seeds (Battaglia et al., 2008) and, it is therefore tempting to speculate that LEA proteins are enrolled in a diurnal, thus short-term, protection against potential temperature or drought stresses in developing seeds.

Global gene expression in barley caryopses suggests different phases of diurnal adaptation to environmental input factors

Finally, we tried to summarize our findings on the predominant functional processes and corresponding genes in Figure 10, which provides a better overview over the network of several interconnected phases of diurnal gene expression.

At the end of the dark phase, depleted pools of sugars and many amino acids as well as low expression of genes involved in phloem unloading, such as *HvCWINV1* and *HvSTP1*(Weschke et al., 2003), are characteristic for a phase of starvation. This is supported by the induced expression of *HvBAM5* as a potential central player in starch degradation. In contrast, during the late light and early dark phases, metabolite pools are saturated and expression of genes related to protein metabolism, storage starch biosynthesis, cell wall expansion, and embryo development are indicative of extensive cell growth and storage compound accumulation (Sets 2 and 3). Interestingly, we see indications for the existence of priming in barley caryopses, as altered gene expression of genes impaired in cellular signaling in Sets 1 and 4 occurred in *anticipation* of dawn and dusk rather than in *response* to changes in light conditions (Davis and Millar, 2001). An involvement of the circadian clock in regulation of gene expression in barley caryopses is further suggested by the expression of a putative ortholog of the potential central circadian regulator gene *LATE ELONGATED HYPOCOTYL* (*LHY1*) (Contig3875_s_at) in Set 1, which was negatively correlated to the evening genes *GIGANTEA* (*GI*) (Contig5247_at) and *PHYTOCLOCK 1/ LUX ARRHYTHMO* (*PCL1/LUX*) (Contig13480_at) (Yakir et al., 2007) contained in Set 4.

During the early light phase and around midday, the induced expression of genes

involved in photosynthesis, and transient starch and fructan biosynthesis prompts the assumption that incoming light signals and metabolite availability regulate gene expression (Sets 5 and 6). Indeed, the biosynthesis of fructans plays an important role in carbon partitioning in leaves by buffering the excess sucrose that is produced during times of maximum photosynthesis (Pollock et al., 2003) and a similar function might exist in caryopses. Expression of heat stress-related genes is typical during the middle of the day and highlights their possible dual roles: on the one hand they are involved in the heat stress response; on the other hand they play roles in general cellular processes as chaperones in higher-order complexes (Bosl et al., 2006; Rajan and D'Silva, 2009). A similar dual functionality for genes related to other stresses has previously been suggested (Kreps et al., 2002).

Conclusions

To the best of our knowledge, this study provides the first global monitoring of diurnal fluctuations in gene expression in a developing cereal seed. On the basis of the experimental work and metadata analysis we conclude that all suborgans are subject to diurnal regulation. This regulation includes processes such as phloem unloading, embryo development, and biosynthesis of storage products, which are independent of the photosynthetic active tissues. Thus in addition to available developmental and spatial gene expression data published by Sreenivasulu et al.(2008) and Radchuk et al.(2009), the diurnal dataset presented here adds a third dimension of complexity to the regulation of gene expression in the barley caryopsis. The combined use of the three available datasets aids the understanding of function and interplay of thousands of genes expressed in a barley seed, which provides a model for other cereal crops.

Materials and Methods

Plant growth, identification of developmental state, harvest and pooling strategies

Barley plants (*Hordeum vulgare*, cultivar Golden Promise) were grown in a greenhouse with automated shading in soil in pots of 10 cm diameter with additional lighting from Xenon light bulbs (15 h light [6:00 AM - 9:00 PM], 9 h dark [9:00 PM - 6:00 AM]; (22°C to 24°C; 40% rel. humidity). The age of caryopses was determined as described by

Weschke et al. (2000). Spikes were labeled at the onset of anthesis and harvested twelve days post anthesis (d.p.a.). Five adjacent caryopses to the spikelet used for determination of age were used for the studies. At each time point, a total of 30 caryopses of spikes from six different plants (5 each) were harvested. Awns, i.e. the projection of the tip of the lemma, and possibly still adhesive anthers were removed from the caryopsis before freezing it in liquid nitrogen. To allow for rapid harvesting (30 seconds per spike) and to avoid induction of wounding induced gene expression, the remaining parts of the husk were not removed from the caryopsis. Caryopses of individual plants were homogenized in liquid nitrogen. Tissue powder of homogenized caryopses of three plants was pooled and used for RNA extraction.

Microarray hybridization

RNA extraction of caryopses was performed as described by Singh et al. (2003). Briefly, 100mg of pooled homogenized plant material was mixed with 900 µl of sarcosyl buffer (1% sodium lauryl sarcosinate, 0.1M Tris-HCl pH 7.5, 0.1 M NaCl, 20 mM EDTA, 50 mM beta-mercaptoethanol) and purification of nucleic acids was done by three steps of phenol-chloroform-isoamylalcohol (25:24:1) extractions. Precipitation of nucleic acids was performed with sodium acetate (pH 5.2) and 1 volume isopropanol. After centrifugation, sediment was washed with ethanol and purified RNA was dissolved in DEPC treated water. Incubation at 65 °C for 5 min, followed by centrifugation at 4 °C was performed to remove residual high molecular weight polysaccharides. The obtained RNA solution was purified following the RNeasy (Quiagen) clean up protocol. RNA quantity and integrity were assessed using RNA 6000 Nano LabChip Kit and the BioAnalyzer software (Agilent).

Two independent samples of 1µg of total RNA were used to synthesize amplified cRNA (MessageAmp™ II aRNA Amplification Kit; Ambion). After fragmentation of cRNA using the RNA Fragmentation Reagents (Ambion), the cRNA was hybridized to Affymetrix Barley1 GeneChips. Hybridization and scanning of the GeneChips was performed according to the manufacturer's instructions.

Data processing

The Affymetrix CEL files were imported into GeneSpring software version 7 (Agilent Technologies). The data discussed in this publication have been deposited in NCBI's Gene Expression Omnibus (Edgar et al., 2002) and are accessible through GEO Series accession number GSE20034 (http://www.ncbi.nlm.nih.gov/geo/query/acc.cgi?acc=GSE20034). Per-Chip normalization to the median was applied to obtain comparability. The arrays were adjusted for background optical noise using sequence dependent robust multi-array averaging (GC-RMA) software and normalized using quantile normalization (Wu et al., 2004).

Identification of DE genes was performed with LIMMA ($p \leq 0.05$) as a part of the R (http://cran.r-project.org/) software package: The GC-RMA summary file, a design matrix and a contrast-matrix has been used as input for LIMMA all-against-all time point comparisons. After fitting, a decide test has been performed. Multiple testing for control of false discovery rate was conducted (Benjamini & Hochberg, 1995). Due to a lack of significant present calls (<34 %), one replicate was removed from the analysis (6:00 AM, replicate A).

A k-means clustering of the DE genes for 6 major clusters was conducted, where clusters converged after 28 iterations. To independently validate the number of k-means clusters, the figure of merit (FOM) has been computed using MeV (Saeed et al., 2003) with varying settings and both, Euclidean distance and Pearson correlation.

The principal component analysis (PCA) was performed with mean centering on DE genes as input. PCA, hierachical clustering and k-means clustering were conducted with GeneSpring software version 7 (Agilent Technologies).

Annotations of the Barley1 GeneChip were updated from the HarvEST database (version 1.73) with a stringency set to a minimum of eleven matching probes (Close et al., 2007).

A functional categorization using GO-terms was performed on the TAIR website using the best BLAST matches for Arabidopsis retrieved from the HarvEST annotation tool. Percentages of all functional categories in the different gene lists were calculated in Excel. For the significant over- or under-representation of a particular GO category, the *p*-values were calculated using the hypergeometric distribution in regular spread sheet

analysis programs. The GO-categories of the universe (all present genes with orthologs to Arabidopsis) were compared to the sampling distribution of the respective gene lists.
The MapMan software version 2.2.0 was used to annotate functional BINs of barley genes. The mapping file for the Barley1 Gene Chip was downloaded from the MapMan website (http://gabi.rzpd.de/projects/MapMan/). Default settings were used to perform an uncorrected Wilcoxon rank test.

Comparison with datasets of barley maturating grains (meta-analysis)

The Affymetrix CEL files GSE9365 (Sreenivasulu et al., 2008) were retrieved from the GEO database at NCBI (http://www.ncbi.nlm.nih.gov/geo/) and imported into the GeneSpring software version 7. The arrays were adjusted for background optical noise using sequence dependent robust multi-array averaging (GC-RMA) software and normalized using quantile normalization. Genes are considered to be expressed in the caryopsis in cases where normalized signal intensities were of 50 or higher in at least one of the time points and one of the tissues.
Evaluation of gene expression in the pericarp, endosperm or embryo was conducted for the '4 and 8 days after anthesis' datasets only. To identify genes that are exclusively expressed in the pericarp, the endosperm or the embryo, we performed a subtractive approach: First, the signal intensities were normalized to the mean expression; Second, all DE genes required at least a three-fold difference from the mean expression in at least one of the time points for each of the tissues independently; Third, the DE genes from all tissues were subsequently subtracted from the expressed genes of the tissue under investigation.

Independently from the above procedures, significantly regulated genes in one of the caryopsis's tissue were identified with LIMMA ($p \leq 0.05$) as a part of the R (http://cran.r-project.org/) software package. Multiple testing for control of false discovery rate was conducted (Benjamini and Hochberg, 1995).
Datasets were derived for each of the different tissues (DE genes and tissue-specific genes) and subsequently compared to our DE genes (Table S8).

Metabolite extraction

For HPLC sample preparation, pooled plant material of three caryopses from two plants was lyophilized. Powdered samples (35mg) were taken up in 400 µl methanol solution (80%), incubated at 60 °C for 10 min and centrifuged at 13,000 x g for 15 min at 4 °C. The resulting supernatant was transferred to a new vial. This extraction procedure was repeated, resulting in a final volume of 1200 µl. The extract was split into two volumes of 600 µl and vacuum-dried (samples A and B). Sample A was used for sugar analysis. The dried pellet was dissolved in 250 µl Milli-Q water and centrifuged (1 min, 13,000 x g, 4 °C). The resulting supernatants were filtrated through a 0.22 µm Millex-GV filter. Tenfold dilutions were used for the measurement of sucrose, fructose, ribose and kestose. One-hundredfold dilutions were used for the measurement of glucose. Sample B was used for amino acid analysis. The dried pellet was resuspended in 138 µl lithium diluent (Pickering laboratories). As an internal standard, 12 µl of a 2.5 mM norleucine solution was used. Samples were centrifuged (1min, 13,000 x g, 4 °C) and resulting supernatants were filtered through 0.22 µm Millex-GV filter.

All samples (A + B) were stored at – 20 °C. Quantification of amino acids and sugars by HPLC was carried out as described by Pilot et al. (2004) and Horak et al. (2008). Metabolite contents of three independent samples were normalized to the median and the standard deviation was calculated. Identification of significant fluctuations in metabolite content was performed with LIMMA ($p \leq 0.05$; $p \leq 0.01$; $p \leq 0.001$) as a part of the R (http://cran.r-project.org/) software package, with raw data of the metabolite levels as input. Next, metabolite data was converted into trajectories over time. A Pearson correlation to the normalized expression profiles was performed to identify genes with a correlation coefficient >0.8.

Quantitative PCR

For detection of transcripts at suborgan resolution, caryopses were harvested at the middle of the day and samples of endosperm, pericarp, husk and embryo were hand-dissected. Caryopses at 8 d.p.a. were used to harvest pericarp samples to enable separation from aleurone layers. All remaining suborgans were harvested at 12 d.p.a..

Material of fifteen caryopses was pooled prior to RNA extraction. RNA was extracted using the Spectrum Plant Total RNA Kit (Sigma-Aldrich). RNA quantity and integrity were assessed as described for microarray hybridization.

For each suborgan, three independent samples of 1 µg RNA were used for reverse transcription with an oligo-dT primer for first strand synthesis and Superscript III RNase-Reverse Transcriptase (Invitrogen). cDNA equivalent to a starting material of 10ng total RNA was amplified in 20 µl reaction volumes using the Dynamo Flash SYBR Green qPCR kit (Finnzymes). All qPCR reactions were carried out in an iQ5 Real-Time PCR Detection System (BioRad) following manufacturer's instructions. Reaction conditions were as follows: Initial denaturation at 95 °C for 7 min, followed by 40 cycles of 95 °C for 10 sec and annealing/extension at 60 °C for 30 sec, followed by final extension at 60 °C for 1 min. A melting curve was obtained by gradually increasing the temperature from 60 °C to 98 °C in steps of 0.5 °C and 10sec ramp time. Forward and reverse primers are listed in Table S8. A cDNA pool of all samples was analyzed for a standard dilution series to monitor the qPCR efficiency for each particular primer pair. Based on a geNorm analysis (Vandesompele et al., 2002), Tubulin, HSP70 and Cyclophilin were chosen as multiple reference genes for further quantification of gene expression. Mathematical operations on qPCR data were performed with regular spread sheet analysis using Microsoft Excel.

Acknowledgements

We like to thank Markus Schmid for support with the microarray hybridizations and Bettina Stadelhofer for excellent help with HPLC analysis. We also like to thank Friederike Ladwig for scientific discussions and critical comments on the manuscript and Tom Martin for proof-reading.

Literature cited

Abebe T, Skadsen RW, Kaeppler HF (2004) Cloning and Identification of Highly Expressed Genes in Barley Lemma and Palea. Crop Sci **44:** 942-950

Ashraf M, Foolad MR (2006) Roles of glycine betaine and proline in improving plant abiotic stress resistance. Environmental and Experimental Botany **59:** 206-216

Baguma Y, Sun C, Boren M, Olsson H, Rosenqvist S, Mutisya J, Rubaihayo PR, Jansson C (2008) Sugar-mediated semidian oscillation of gene expression in the cassava storage root regulates starch synthesis. Plant Signal Behav **3:** 439-445

Balmer Y, Vensel WH, Cai N, Manieri W, Schurmann P, Hurkman WJ, Buchanan BB (2006) A complete ferredoxin/thioredoxin system regulates fundamental processes in amyloplasts. Proc Natl Acad Sci U S A **103:** 2988-2993

Battaglia M, Olvera-Carrillo Y, Garciarrubio A, Campos F, Covarrubias AA (2008) The enigmatic LEA proteins and other hydrophilins. Plant Physiol **148:** 6-24

Benjamini Y, Hochberg Y (1995) Controlling the False Discovery Rate: A Practical and Powerful Approach to Multiple Testing. J Roy Statist Soc Ser B **57:** 289-300

Blasing OE, Gibon Y, Gunther M, Hohne M, Morcuende R, Osuna D, Thimm O, Usadel B, Scheible WR, Stitt M (2005) Sugars and circadian regulation make major contributions to the global regulation of diurnal gene expression in Arabidopsis. Plant Cell **17:** 3257-3281

Borisjuk L, Rolletschek H, Radchuk R, Weschke W, Wobus U, Weber H (2004) Seed development and differentiation: A role for metabolic regulation. Plant Biology **6:** 375-386

Bosl B, Grimminger V, Walter S (2006) The molecular chaperone Hsp104--a molecular machine for protein disaggregation. J Struct Biol **156:** 139-148

Burton RA, Jenner H, Carrangis L, Fahy B, Fincher GB, Hylton C, Laurie DA, Parker M, Waite D, van Wegen S, Verhoeven T, Denyer K (2002) Starch granule initiation and growth are altered in barley mutants that lack isoamylase activity. Plant J **31:** 97-112

Burton RA, Zhang XQ, Hrmova M, Fincher GB (1999) A single limit dextrinase gene is expressed both in the developing endosperm and in germinated grains of barley. Plant Physiol **119:** 859-871

Chatterjee M, Berbezy P, Vyas D, Coates S, Barsby T (2004) Reduced expression of a protein homologous to glycogenin leads to reduction of starch content in Arabidopsis leaves. Plant Science **168:** 501-509

Close TJ, Wanamaker S, Roose ML, Lyon M (2007) HarvEST: An EST Database and Viewing Software. Methods Mol Biol **406:** 161-178

Close TJ, Wanamaker SI, Caldo RA, Turner SM, Ashlock DA, Dickerson JA, Wing RA, Muehlbauer GJ, Kleinhofs A, Wise RP (2004) A new resource for cereal genomics: 22K barley GeneChip comes of age. Plant Physiology **134:** 960-968

Contento AL, Kim SJ, Bassham DC (2004) Transcriptome profiling of the response of Arabidopsis suspension culture cells to Suc starvation. Plant Physiol **135:** 2330-2347

Coruzzi GM, Zhou L (2001) Carbon and nitrogen sensing and signaling in plants: emerging 'matrix effects'. Current Opinion in Plant Biology **4:** 247-253

Davis SJ, Millar AJ (2001) Watching the hands of the Arabidopsis biological clock. Genome Biol **2:** REVIEWS1008

Dian W, Jiang H, Chen Q, Liu F, Wu P (2003) Cloning and characterization of the granule-bound starch synthase II gene in rice: gene expression is regulated by the nitrogen level, sugar and circadian rhythm. Planta **218:** 261-268

Edgar R, Domrachev M, Lash AE (2002) Gene Expression Omnibus: NCBI gene expression and hybridization array data repository. Nucleic Acids Res **30:** 207-210

Edner C, Li J, Albrecht T, Mahlow S, Hejazi M, Hussain H, Kaplan F, Guy C, Smith SM, Steup M, Ritte G (2007) Glucan, water dikinase activity stimulates breakdown of starch granules by plastidial beta-amylases. Plant Physiol **145:** 17-28

Endler A, Meyer S, Schelbert S, Schneider T, Weschke W, Peters SW, Keller F, Baginsky S, Martinoia E, Schmidt UG (2006) Identification of a vacuolar sucrose transporter in barley and arabidopsis mesophyll cells by a tonoplast proteomic approach. Plant Physiology **141:** 196-207

Engel N, van den Daele K, Kolukisaoglu U, Morgenthal K, Weckwerth W, Parnik T, Keerberg O, Bauwe H (2007) Deletion of glycine decarboxylase in Arabidopsis is lethal under nonphotorespiratory conditions. Plant Physiol **144:** 1328-1335

Fulton DC, Stettler M, Mettler T, Vaughan CK, Li J, Francisco P, Gil M, Reinhold H, Eicke S, Messerli G, Dorken G, Halliday K, Smith AM, Smith SM, Zeeman SC (2008) Beta-AMYLASE4, a noncatalytic protein required for starch breakdown, acts upstream of three active beta-amylases in Arabidopsis chloroplasts. Plant Cell **20:** 1040-1058

Geigenberger P, Stitt M (2000) Diurnal changes in sucrose, nucleotides, starch synthesis and AGPS transcript in growing potato tubers that are suppressed by decreased expression of sucrose phosphate synthase. Plant J **23:** 795-806

Gomez LD, Baud S, Graham IA (2005) Metabolite sensing in plants: a role for trehalose metabolism in seed development and embryo development. Febs Journal **272:** 460-460

Guerin J, Carbonero P (1997) The Spatial Distribution of Sucrose Synthase Isozymes in Barley. Plant Physiol **114:** 55-62

Gutierrez L, Van Wuytswinkel O, Castelain M, Bellini C (2007) Combined networks regulating seed maturation. Trends Plant Sci **12:** 294-300

Gutierrez RA, Stokes TL, Thum K, Xu X, Obertello M, Katari MS, Tanurdzic M, Dean A, Nero DC, McClung CR, Coruzzi GM (2008) Systems approach identifies an organic nitrogen-responsive gene network that is regulated by the master clock control gene CCA1. Proc Natl Acad Sci U S A **105:** 4939-4944

Hannah LC, James M (2008) The complexities of starch biosynthesis in cereal endosperms. Curr Opin Biotechnol **19:** 160-165

Hannappel U, Vicente-Carbajosa J, Barker JH, Shewry PR, Halford NG (1995) Differential expression of two barley SNF1-related protein kinase genes. Plant Mol Biol **27:** 1235-1240

Hejazi M, Fettke J, Haebel S, Edner C, Paris O, Frohberg C, Steup M, Ritte G (2008) Glucan, water dikinase phosphorylates crystalline maltodextrins and thereby initiates solubilization. Plant J **55:** 323-334

Hoch G (2007) Cell wall hemicelluloses as mobile carbon stores in non-reproductive plant tissues. Functional Ecology **21:** 823-834

Horak J, Grefen C, Berendzen KW, Hahn A, Stierhof YD, Stadelhofer B, Stahl M, Koncz C, Harter K (2008) The Arabidopsis thaliana response regulator ARR22 is a putative AHP phospho-histidine phosphatase expressed in the chalaza of developing seeds. BMC Plant Biol **8:** 77

Johnson PE, Patron NJ, Bottrill AR, Dinges JR, Fahy BF, Parker ML, Waite DN, Denyer K (2003) A low-starch barley mutant, riso 16, lacking the cytosolic small subunit of ADP-glucose pyrophosphorylase, reveals the importance of the cytosolic isoform and the identity of the plastidial small subunit. Plant Physiol **131:** 684-696

Koch KE (1996) Carbohydrate-modulated gene expression in plants. Annual Review Of Plant Physiology And Plant Molecular Biology **47:** 509-540

Kotting O, Pusch K, Tiessen A, Geigenberger P, Steup M, Ritte G (2005) Identification of a novel enzyme required for starch metabolism in Arabidopsis leaves. The phosphoglucan, water dikinase. Plant Physiol **137:** 242-252

Kreps JA, Wu YJ, Chang HS, Zhu T, Wang X, Harper JF (2002) Transcriptome changes for Arabidopsis in response to salt, osmotic, and cold stress. Plant Physiology **130:** 2129-2141

Lam HM, Coschigano K, Schultz C, Melo-Oliveira R, Tjaden G, Oliveira I, Ngai N, Hsieh MH, Coruzzi G (1995) Use of Arabidopsis mutants and genes to study amide amino acid biosynthesis. Plant Cell **7:** 887-898

Lam HM, Wong P, Chan HK, Yam KM, Chen L, Chow CM, Coruzzi GM (2003) Overexpression of the ASN1 gene enhances nitrogen status in seeds of Arabidopsis. Plant Physiol **132:** 926-935

Lee EJ, Matsumura Y, Soga K, Hoson T, Koizumi N (2007) Glycosyl hydrolases of cell wall are induced by sugar starvation in Arabidopsis. Plant Cell Physiol **48:** 405-413

Li S, Qian Q, Fu Z, Zeng D, Meng X, Kyozuka J, Maekawa M, Zhu X, Zhang J, Li J, Wang Y (2009) Short panicle1 encodes a putative PTR family transporter and determines rice panicle size. Plant J **58:** 592-605

Li Z, Sun F, Xu S, Chu X, Mukai Y, Yamamoto M, Ali S, Rampling L, Kosar-Hashemi B, Rahman S, Morell MK (2003) The structural organisation of the gene encoding class II starch synthase of wheat and barley and the evolution of the genes encoding starch synthases in plants. Funct Integr Genomics **3:** 76-85

Lothier J, Lasseur B, Le Roy K, Van Laere A, Prud'homme MP, Barre P, Van den Ende W, Morvan-Bertrand A (2007) Cloning, gene mapping, and functional analysis of a fructan 1-exohydrolase (1-FEH) from Lolium perenne implicated in fructan synthesis rather than in fructan mobilization. J Exp Bot **58:** 1969-1983

Lu Y, Gehan JP, Sharkey TD (2005) Daylength and circadian effects on starch degradation and maltose metabolism. Plant Physiol **138:** 2280-2291

Maeda K, Finnie C, Ostergaard O, Svensson B (2003) Identification, cloning and characterization of two thioredoxin H isoforms, HvTrxh1 and HvTrxh2, from the barley seed proteome. European Journal Of Biochemistry **270:** 2633-2643

Mangelsen E, Kilian J, Berendzen KW, Kolukisaoglu UH, Harter K, Jansson C, Wanke D (2008) Phylogenetic and comparative gene expression analysis of

barley (Hordeum vulgare) WRKY transcription factor family reveals putatively retained functions between monocots and dicots. BMC Genomics **9:** 194

Michael TP, Mockler TC, Breton G, McEntee C, Byer A, Trout JD, Hazen SP, Shen R, Priest HD, Sullivan CM, Givan SA, Yanovsky M, Hong F, Kay SA, Chory J (2008) Network discovery pipeline elucidates conserved time-of-day-specific cis-regulatory modules. PLoS Genet **4:** e14

Miranda M, Borisjuk L, Tewes A, Dietrich D, Rentsch D, Weber H, Wobus U (2003) Peptide and amino acid transporters are differentially regulated during seed development and germination in faba bean. Plant Physiol **132:** 1950-1960

Nagaraj VJ, Altenbach D, Galati V, Lüscher M, Meyer AD, Boller T, Wiemken A (2004) Distinct regulation of sucrose: sucrose-1-fructosyltransferase (1-SST) and sucrose: fructan-6-fructosyltransferase (6-SFT), the key enzymes of fructan synthesis in barley leaves: 1-SST as the pacemaker. New Phytol **161:** 735-748

Nagaraj VJ, Galati V, Lüscher M, Boller T, Wiemken A (2005) Cloning and functional characterization of a cDNA encoding barley soluble acid invertase (HvINV1). Plant Science **168:** 249-258

Osuna D, Usadel B, Morcuende R, Gibon Y, Blasing OE, Hohne M, Gunter M, Kamlage B, Trethewey R, Scheible WR, Stitt M (2007) Temporal responses of transcripts, enzyme activities and metabolites after adding sucrose to carbon-deprived Arabidopsis seedlings. Plant J **49:** 463-491

Patrick JW, Offler CE (2001) Compartmentation of transport and transfer events in developing seeds. Journal of Experimental Botany **52:** 551-564

Patron NJ, Greber B, Fahy BF, Laurie DA, Parker ML, Denyer K (2004) The lys5 mutations of barley reveal the nature and importance of plastidial ADP-Glc transporters for starch synthesis in cereal endosperm. Plant Physiol **135:** 2088-2097

Patron NJ, Smith AM, Fahy BF, Hylton CM, Naldrett MJ, Rossnagel BG, Denyer K (2002) The altered pattern of amylose accumulation in the endosperm of low-amylose barley cultivars is attributable to a single mutant allele of granule-bound starch synthase I with a deletion in the 5'-non-coding region. Plant Physiol **130:** 190-198

Paul MJ, Pellny TK (2003) Carbon metabolite feedback regulation of leaf photosynthesis and development. J Exp Bot **54:** 539-547

Pego JV, Kortstee AJ, Huijser C, Smeekens SC (2000) Photosynthesis, sugars and the regulation of gene expression. J Exp Bot **51 Spec No:** 407-416

Perez-Lopez U, Robredo A, Lacuesta M, Sgherri C, Munoz-Rueda A, Navari-Izzo F, Mena-Petite A (2009) The oxidative stress caused by salinity in two barley cultivars is mitigated by elevated CO2. Physiol Plant **135:** 29-42

Pilot G, Stransky H, Bushey DF, Pratelli R, Ludewig U, Wingate VP, Frommer WB (2004) Overexpression of GLUTAMINE DUMPER1 leads to hypersecretion of glutamine from Hydathodes of Arabidopsis leaves. Plant Cell **16:** 1827-1840

Pollock C, Farrar J, Tomos D, Gallagher J, Lu CG, Koroleva O (2003) Balancing supply and demand: the spatial regulation of carbon metabolism in grass and cereal leaves. Journal Of Experimental Botany **54:** 489-494

Pratelli R, Pilot G (2007) Altered amino Acid metabolism in glutamine dumper1 plants. Plant Signal Behav **2:** 182-184

Radchuk VV, Borisjuk L, Sreenivasulu N, Merx K, Mock HP, Rolletschek H, Wobus U, Weschke W (2009) Spatiotemporal profiling of starch biosynthesis and degradation in the developing barley grain. Plant Physiol **150:** 190-204

Rajan VB, D'Silva P (2009) Arabidopsis thaliana J-class heat shock proteins: cellular stress sensors. Funct Integr Genomics **9:** 433-446

Ramon M, I DES, Vandesteene L, Naudts M, Leyman B, P VAND, Rolland F, Beeckman T, Thevelein JM (2009) Extensive expression regulation and lack of heterologous enzymatic activity of the Class II trehalose metabolism proteins from Arabidopsis thaliana. Plant Cell Environ

Rolland F, Baena-Gonzalez E, Sheen J (2006) Sugar sensing and signaling in plants: conserved and novel mechanisms. Annu Rev Plant Biol **57:** 675-709

Sabelli PA, Larkins BA (2009) The development of endosperm in grasses. Plant Physiol **149:** 14-26

Saeed AI, Sharov V, White J, Li J, Liang W, Bhagabati N, Braisted J, Klapa M, Currier T, Thiagarajan M, Sturn A, Snuffin M, Rezantsev A, Popov D, Ryltsov A, Kostukovich E, Borisovsky I, Liu Z, Vinsavich A, Trush V, Quackenbush J (2003) TM4: a free, open-source system for microarray data management and analysis. Biotechniques **34:** 374-378

Sanders A, Collier R, Trethewy A, Gould G, Sieker R, Tegeder M (2009) AAP1 regulates import of amino acids into developing Arabidopsis embryos. Plant J **59:** 540-552

Shahpiri A, Svensson B, Finnie C (2008) The NADPH-dependent thioredoxin reductase/thioredoxin system in germinating barley seeds: gene expression, protein profiles, and interactions between isoforms of thioredoxin h and thioredoxin reductase. Plant Physiol **146:** 789-799

Singh G, Kumar S, Singh P (2003) A quick method to isolate RNA from wheat and other carbohydrate-rich seeds. Plant Molecular Biology Reporter **21:** 93a-93f

Smith AM (1999) Making starch. Current Opinion In Plant Biology **2:** 223-229

Smith AM (2001) The biosynthesis of starch granules. Biomacromolecules **2:** 335-341

Smith AM, Stitt M (2007) Coordination of carbon supply and plant growth. Plant Cell Environ **30:** 1126-1149

Smith AM, Zeeman SC, Smith SM (2005) Starch degradation. Annu Rev Plant Biol **56:** 73-98

Sreenivasulu N, Radchuk V, Strickert M, Miersch O, Weschke W, Wobus U (2006) Gene expression patterns reveal tissue-specific signaling networks controlling programmed cell death and ABA- regulated maturation in developing barley seeds. Plant J **47:** 310-327

Sreenivasulu N, Usadel B, Winter A, Radchuk V, Scholz U, Stein N, Weschke W, Strickert M, Close TJ, Stitt M, Graner A, Wobus U (2008) Barley Grain Maturation and Germination: Metabolic Pathway and Regulatory Network Commonalities and Differences Highlighted by New MapMan/PageMan Profiling Tools. Plant Physiol **146:** 1738-1758

Streb S, Delatte T, Umhang M, Eicke S, Schorderet M, Reinhardt D, Zeeman SC (2008) Starch granule biosynthesis in Arabidopsis is abolished by removal of all debranching enzymes but restored by the subsequent removal of an endoamylase. Plant Cell **20:** 3448-3466

Sun CX, Palmqvist S, Olsson H, Boren M, Ahlandsberg S, Jansson C (2003) A novel WRKY transcription factor, SUSIBA2, participates in sugar signaling in barley by binding to the sugar-responsive elements of the iso1 promoter. Plant Cell **15:** 2076-2092

Sun CX, Sathish P, Ahlandsberg S, Deiber A, Jansson C (1997) Identification of four starch-branching enzymes in barley endosperm: partial purification of forms I, IIa and IIb. New Phytologist **137:** 215-222

Sun CX, Sathish P, Ahlandsberg S, Jansson C (1998) The two genes encoding starch-branching enzymes IIa and IIb are differentially expressed in barley. Plant Physiology **118:** 37-49

Sun CX, Sathish P, Ahlandsberg S, Jansson C (1999) Analyses of isoamylase gene activity in wild-type barley indicate its involvement in starch synthesis. Plant Molecular Biology **40:** 431-443

Thiel J, Weier D, Sreenivasulu N, Strickert M, Weichert N, Melzer M, Czauderna T, Wobus U, Weber H, Weschke W (2008) Different hormonal regulation of cellular differentiation and function in nucellar projection and endosperm transfer cells: a microdissection-based transcriptome study of young barley grains. Plant Physiol **148:** 1436-1452

Thimm O, Blasing O, Gibon Y, Nagel A, Meyer S, Kruger P, Selbig J, Muller LA, Rhee SY, Stitt M (2004) MAPMAN: a user-driven tool to display genomics data sets onto diagrams of metabolic pathways and other biological processes. Plant J **37:** 914-939

Thorbjornsen T, Villand P, Kleczkowski LA, Olsen OA (1996) A single gene encodes two different transcripts for the ADP-glucose pyrophosphorylase small subunit from barley (Hordeum vulgare). Biochem J **313 (Pt 1):** 149-154

Tzafrir I, Pena-Muralla R, Dickerman A, Berg M, Rogers R, Hutchens S, Sweeney TC, McElver J, Aux G, Patton D, Meinke D (2004) Identification of genes required for embryo development in Arabidopsis. Plant Physiol **135:** 1206-1220

Usadel B, Blasing OE, Gibon Y, Retzlaff K, Hohne M, Gunther M, Stitt M (2008) Global transcript levels respond to small changes of the carbon status during progressive exhaustion of carbohydrates in Arabidopsis rosettes. Plant Physiol **146:** 1834-1861

Van Den Ende W, Clerens S, Vergauwen R, Van Riet L, Van Laere A, Yoshida M, Kawakami A (2003) Fructan 1-exohydrolases. beta-(2,1)-trimmers during graminan biosynthesis in stems of wheat? Purification, characterization, mass mapping, and cloning of two fructan 1-exohydrolase isoforms. Plant Physiol **131:** 621-631

Vandesompele J, De Preter K, Pattyn F, Poppe B, Van Roy N, De Paepe A, Speleman F (2002) Accurate normalization of real-time quantitative RT-PCR data by geometric averaging of multiple internal control genes. Genome Biol **3:** RESEARCH0034

Vijn I, Smeekens S (1999) Fructan: More than a reserve carbohydrate? Plant Physiology **120:** 351-359

Villand P, Olsen OA, Kilian A, Kleczkowski LA (1992) ADP-Glucose Pyrophosphorylase Large Subunit cDNA from Barley Endosperm. Plant Physiol **100:** 1617-1618

Weigelt K, Kuster H, Radchuk R, Muller M, Weichert H, Fait A, Fernie AR, Saalbach I, Weber H (2008) Increasing amino acid supply in pea embryos reveals specific interactions of N and C metabolism, and highlights the importance of mitochondrial metabolism. Plant J **55:** 909-926

Weschke W, Panitz R, Gubatz S, Wang Q, Radchuk R, Weber H, Wobus U (2003) The role of invertases and hexose transporters in controlling sugar ratios in maternal and filial tissues of barley caryopses during early development. Plant Journal **33:** 395-411

Weschke W, Panitz R, Sauer N, Wang Q, Neubohn B, Weber H, Wobus U (2000) Sucrose transport into barley seeds: molecular characterization of two transporters and implications for seed development and starch accumulation. Plant Journal **21:** 455-467

Wijnen H, Young MW (2006) Interplay of circadian clocks and metabolic rhythms. Annu Rev Genet **40:** 409-448

Wu Z, Irizarry RA, Gentleman R, Martinez Murillo F, Spencer F (2004) A model based background adjustment for oligonucleotide expression arrays. Berkeley Electronic Press **1001**

Yakir E, Hilman D, Harir Y, Green RM (2007) Regulation of output from the plant circadian clock. FEBS J **274:** 335-345

Zeeman SC, Smith SM, Smith AM (2007) The diurnal metabolism of leaf starch. Biochem J **401:** 13-28

Zheng ZL (2009) Carbon and nitrogen nutrient balance signaling in plants. Plant Signal Behav **4:** 584-591

Figure legends

Figure 1. Sampling of plant material and profiles of differentially expressed genes. A, Central region of a barley spike. One floret was removed to determine the onset of flowering. At 12 days post anthesis (d.p.a.) the five barley caryopses closest to the floret used for determination of the onset of anthesis were harvested (white asterisks). B, Prior to pooling and freezing the samples, awns and possibly remaining anthers were removed from the caryopses. C, Expression profile of 2,091 differentially expressed (DE) genes during the diurnal cycle. Six time points of harvest in dark and light phase are indicated at the x-axis as follows: beginning and end of the dark phase (1h and 9h), beginning of the light phase (10h), middle of the light phase (17 and 20h) and end of the light phase (23h).

Figure 2. Expression patterns of k-means clusters of DE genes and their classification into functional categories of Gene Ontology (GO). A, Gene expression trajectories of the k-means clusters named Set 1 to 6. The respective six time points are indicated at the x-axis. Total numbers of assigned probesets are given in parentheses. Colors of the profiles depict the normalized transcript level of the probeset at 1h: red, high expression; yellow, moderate expression; blue, low expression. B, Classification of genes according to GO groups for Biological Processes. The number of genes belonging to a particular GO group is shown as percentage for all present probesets detected by the microarray (17,416 expressed), all DE genes (2,091 genes) and the subsets of genes belonging to clusters 1 to 6 (Set 1 to Set 6). Asterisks indicate a significant over- or underrepresentation of functional categories compared to the functional categories of all expressed genes with putative orthologs in Arabidopsis (* $p \leq 0.01$; ** $p \leq 0.001$; *** $p \leq 0.0001$).

Figure 3. MapMan display showing diurnal amplitudes of 17,416 present genes in a metabolism overview map. Genes on the Barley1 microarray are represented by individual squares. Genes with increasingly large amplitudes are shown as an increasingly intense blue saturating at an amplitude of 1.3 ($\log_2$-value). Genes with no significant change in the amplitude are shown in white. Abbreviations used in the Figure: TCA, tricarboxylic acid; CHO, carbohydrate; OPP, oxidative pentose phosphate.

Figure 4. Levels of sugars and amino acids undergo diurnal fluctuations in developing caryopses of barley. A, The amount of sugars was determined at six times during the day. B, C and D, The amount of indicated amino acids was determined at six times during the day. Sampling times were as indicated for the glucose samples in A. Grey and light blue bars depict times in darkness and light, respectively. The data are displayed as mean plus standard deviation. Significant differences compared to the first sample (1h) are indicated by asterisks (*$p \leq 0.01$; ** $p \leq 0.001$; *** $p \leq 0.0001$).

Figure 5. Correlation of sugar contents and expression profiles. Profiles of the indicated sugars and their correlating and anti-correlating gene expression profiles are shown as pink or black lines, respectively. Time points are indicated at the x-axis. Numbers of correlating genes are displayed for each of the diagrams. Sugar contents and signal intensities are normalized to the mean and plotted in log-scale.

Figure 6. Correlation of amino acid contents and expression profiles. Profiles of the indicated amino acids and their correlating and anti-correlating gene expression profiles are shown as blue or black lines, respectively. Numbers of correlating genes are displayed for each of the diagrams, time points are indicated at the bottom. The amino acid contents and signal intensities are normalized to the mean and plotted in log-scale.

Figure 7. Gene expression profiles of genes involved in sugar metabolism and signaling. Signal intensities at indicated time points during the day are normalized to the mean expression values and plotted in log-scale. Genes are grouped based on their involvement in different pathways as follows: Initial sugar transport and processing (A), starch and fructan synthesis and degradation (B,C)potential sugar signaling (D) and ferredoxin/thioredoxin system (E),. DE genes are indicated by asterisks. For complete gene names please refer to Table 1.

Figure 8. Diurnal gene expression in suborgan tissues of the caryopses. (A) The total number of genes that were expressed in the suborgans pericarp, endosperm and embryo

are shown in blue, red and yellow, respectively. Subsets of genes that were exclusively expressed in one suborgan are shown in light-shaded colors. Diurnally expressed genes are depicted in dark-shaded colors. (B) Venn diagrams depicting the exclusive and interference of suborgan-specific and diurnally regulated genes.

Figure 9. Presence of transcripts in four different tissues of the developing barley caryopsis. Normalized transcript abundance of selected genes were determined by qPCR. Expression levels in endosperm, pericarp, husk and embryo tissues are shown. Results are displayed for genes coding for the following proteins: WRKY transcription factor 41 (*HvWRKY41*), beta-Amylase 5 (*HvBAM5*), Isoamylase 1 (*HvISA1*), Glucan Water Dikinase 1 (*HvGWD1*), Isoamylase 3 (*HvISA3*), Plant Glycogenin-like Starch Initiation Protein 1 (*HvPGSIP1*), Isoamylase 2 (*HvISA2*), Plant Glycogenin-like Starch Initiation Protein 2 (*HvPGSIP2*), Limit Dextrinase (*HvLD*) and WRKY transcription factor SUSIBA2 (*HvWRKY46*).

Figure 10. Schematic overview of the diurnal expressional trends in developing caryopses of barley. Functional groups of DE genes with high transcript levels at the investigated times of the day, summarized as morning, midday and evening, are depicted as blue boxes. The length of the blue boxes is indicative for the duration of high expression levels over just one or several investigated time points that are indicated at the bottom of the model. Five phases of diurnal adaptation, named starvation & priming, energy collection & carbon fixation, light protection & chaperone activity, storage & growth, and embryo development, were defined and are indicated in italics. White and grey areas depict light and dark phases of the day, respectively. TF, Transcription factors; LEA, Late embryo abundant proteins; EMB, Embryo defective proteins.

Table 1. Genes investigated in this study with known or putative involvement in sugar signaling and sucrose to starch conversion.

Protein name	Gene [a]	Barley1 probeset	DE[b]	Organ[c]	Fold[d]	Reference
ADP-Glc pyrophosphorylase large subunit	*HvAPL1*	Contig3390_at	(1)	U	1.83	(Villand et al., 1992)
ADP-Glc pyrophosphorylase large subunit	*HvAPL2*	Contig5267_at	No	U	1.37	(Villand et al., 1992)
ADP-Glc pyrophosphorylase small subunit	*HvAPS1a/b*	Contig2267_s_at	No	U	1.35	(Thorbjornsen et al., 1996)
ADP-Glc pyrophosphorylase small subunit	*HvAPS2*	*No probeset*		U		(Johnson et al., 2003)
ADP-glucose transporter	*HvNST1*	Contig7529_at	(6)	U	2.39	(Patron et al., 2004)
Alpha-Amylase 1	*HvAMY1*	Contig7088_at	*n.d.*	U		(Radchuk et al., 2009)
Alpha-Amylase 2	*HvAMY2*	Contig3952_at	*n.d*	*n.d.*		(Radchuk et al., 2009)
Alpha-Amylase 3	*HvAMY3*	Contig3953_s_at	No	*n.d.*	1.12	(Radchuk et al., 2009)
Alpha-Amylase 4	*HvAMY4*	EBma03_SQ002_M07_at	No	P	1.35	(Radchuk et al., 2009)
Alpha-glucan phosphorylase,	*HvPHO1*	No probeset		U		(Radchuk et al., 2009)
Alpha-glucan phosphorylase, cytosolic	*HvPHO2*	Contig6517_at		U	0.50	(Radchuk et al., 2009)
Beta Amylase 1	*HvBAM1*	Contig1406_at	No	U	1.41	(Radchuk et al., 2009)
Beta-Amylase 2	*HvBAM2*	Contig1411_s_at	No	U	1.34	(Radchuk et al., 2009)
Beta-Amylase 3	*HvBAM3*	Contig8246_at	*n.d.*	U		(Radchuk et al., 2009)
Beta-Amylase 4	*HvBAM4*	*No probeset*		U		(Radchuk et al., 2009)
Beta-Amylase 5	*HvBAM5*	Contig11522_at	(1)	U	5.21	(Radchuk et al., 2009)
Beta-Amylase 6	*HvBAM6*	*No probeset*		U		(Radchuk et al., 2009)
Beta-Amylase7	*HvBAM7*	*No probeset*		U		(Radchuk et al., 2009)
Beta-Amylase 8	*HvBAM8*	Contig10917_at	No	U	1.38	(Edner et al., 2007)
Cell wall invertase 1	*HvCWINV1*	Contig11241_at	(3)	U	2.28	(Weschke et al., 2003)
Cell wall invertase 2	*HvCWINV2*	Contig6787_at	No	U	1.48	(Weschke et al., 2003)
Disproportionating Enzyme 1	*HvDPE1*	Contig26451_at	No	U	1.49	(Radchuk et al., 2009)
Disproportionating Enzyme 2	*HvDPE2*	Contig6654_at	No	U	1.48	(Radchuk et al., 2009)
Ferredoxin-NADP reductase, putative	*FNR1-like*	baak21d06_s_at	(4)	U	1.96	
Ferredoxin-thioredoxin reductase, putative	*FTR-like*	Contig14916_at	No	P	1.16	(Patron et al., 2004)
Fructan 1-exohydrolase	*Hv1-FEH*	Contig7811_s_at	(3)	U	2.21	(Nagaraj et al., 2004)
Glucan Water Dikinase 1	*HvGWD1*	Contig18313_at	(4)	U	2.08	(Edner et al., 2007)
Glucan Water Dikinase 2	*HvGWD2*	Contig14761_at	*n.d.*	U		(Edner et al., 2007)
Granule bound starch synthase 1a	*HvGBSS1a*	Contig694_at	No	U	1.32	(Patron et al., 2002)
Granule bound starch synthase 1b	*HvGBSS1b*	Contig12208_at	(4)	U	1.80	(Patron et al., 2002)
Hexokinase 1	*HvHXK1*	Contig12296_at	(2)	P	1.72	(Mangelsen, unpublished)
Hexokinase 2	*HvHXK2*	Contig17401_at	No	P	1.42	(Mangelsen, unpublished)
Hexokinase 3	*HvHXK3*	Contig14657_at	No	U	1.38	(Mangelsen, unpublished)
Hexokinase 5	*HvHXK5*	Contig4153_at	No	U	1.20	(Mangelsen, unpublished)
Isoamylase 1	*HvISA1*	Contig7560_at	No	P	1.11	(Sun et al., 1999)
Isoamylase 2	*HvISA2*	Contig13547_at	No	E	1.24	(Radchuk et al., 2009)
Isoamylase 3	*HvISA3*	Contig14990_at	(6)	U	1.38	(Radchuk et al., 2009)
Limit Dextrinase (Pullulanase)	*HvLD*	Contig11648_at	(3)	U	1.86	(Burton et al., 1999)
NADPH-dependent thioredoxin reductase 2	*HvNTR2*	HB22M22r_s_at	No	U	1.50	(Shahpiri et al., 2008)
Phosphoglucan, water dikinase	*HvPWD*	*No probeset*		U		(Kotting et al., 2005)

Plant Glycogenin like Starch Initiation Protein 1	*HvPGSIP1*	rbags11k20_s_at	No	U	1.28	(Chatterjee et al., 2004)
Plant Glycogenin like Starch Initiation Protein2	*HvPGSIP2*	Contig3977_at	(3)	U	4.01	(Chatterjee et al., 2004)
SNF1-related protein kinase a	*HvSnRK1a*	Contig3529_at	No	E	1.33	(Hannappel et al., 1995)
SNF1-related protein kinase b	*HvSnRK1b*	HVSMEc0011O22r2_at	No	U	1.54	(Hannappel et al., 1995)
Starch branching enzyme I	*HvSBEI*	*No probeset*		U		(Sun et al., 1997)
Starch branching enzyme IIa	*HvSBEIIa*	Contig3761_at	No	U	1.42	(Sun et al., 1998)
Starch branching enzyme IIb	*HvSBEIIb*	Contig3762_s_at	(5)	E		(Sun et al., 1998)
Starch Synthase I	*HvSSI*	Contig1808_at	No	U	1.59	(Li et al., 2003)
Starch Synthase IIa	*HvSSIIa*	Contig20469_at	No	U	1.85	(Li et al., 2003)
Starch Synthase IIb	*HvSSIIb*	*No probeset*		U		(Radchuk et al., 2009)
Starch Synthase IIIa	*HvSSIIIa*	*No probeset*		U		(Radchuk et al., 2009)
Starch Synthase IIIb	*HvSSIIIb*	Contig10722_at	(6)	U	2.96	(Radchuk et al., 2009)
Starch Synthase IV	*HvSSIV*	Contig13138_at	No	U	1.26	(Radchuk et al., 2009)
Sucrose synthase 1	*HvSuSy1*	Contig361_s_at	No	U	2.05	(Guerin and Carbonero, 1997)
Sucrose synthase 2	*HvSuSy2*	Contig823_at	No	U	1.40	(Guerin and Carbonero, 1997)
Sucrose transporter 1	*HvSUT1*	Contig4612_at	No	U	1.44	(Weschke et al., 2000)
Sucrose transporter 2	*HvSUT2*	rbah43d09_s_at	(3)	U	1.66	(Weschke et al., 2000)
Sucrose: fructan-6-fructosyltransferase	*Hv6-SFT*	Contig3392_at	(4)	U	2.64	(Nagaraj et al., 2004)
Sucrose: sucrose-1-fructosyltransferase	*Hv1-SST*	Contig4521_s_at	No	U	1.41	(Nagaraj et al., 2004)
Sugar transporter 1	*HvSTP1*	Contig3479_at	(5)	U	1.91	(Weschke et al., 2003)
Sugar transporter 2	*HvSTP2*	*No probeset*		U		(Weschke et al., 2003)
Sugar transporter 3	*HvSTP3*	Contig6135_s_at	No	U	1.26	(Weschke et al., 2003)
Thioredoxin *f*	*Trx f-like*	Contig4022_at	(6)	U	4.06	
Thioredoxin *h 1*	*HvTrx h1*	Contig171_at	No	P	1.38	(Maeda et al., 2003)
Thioredoxin *h 2*	*HvTrx h2*	Contig2980_s_at	No	P	1.09	(Maeda et al., 2003)
Thioredoxin *h,* putative	*Trx h-like*	HV06G09u_s_at	(6)	P	1.63	(Maeda et al., 2003)
Thioredoxin *m,* putative	*Trx m-like*	Contig26351_at	(3)	E	2.09	
Thioredoxin-like 1	*Trx-like 1*	Contig5236_at	(6)	U	2.15	
Trehalose-6-Phosphate Phosphatase, putative	*TPP-like*	HS16E24u_s_at	(3)	U	2.81	(Ramon et al., 2009)
Trehalose-6-Phosphate Synthase, putative	*TPS-like*	Contig3373_s_at	(6)	U	2.14	(Ramon et al., 2009)
WRKY Transcription Factor 34	*HvWRKY34*	Contig10471_at	No	U	1.61	(Mangelsen et al., 2008)
WRKY Transcription Factor 41	*HvWRKY41*	Contig12033_at	(3)	U	1.78	(Mangelsen et al., 2008)
WRKY Transcription Factor Susiba2	*HvWRKY46*	Contig7243_at	No	U	1.10	(Sun et al., 2003)

[a] Previously annotated barley genes carry the prefix "Hv"; gene annotations based on best BLAST matches in Arabidopsis or rice carry the suffix "-like"

[b] Differential Expression according to the calculation of 2,091 DE probesets. Number of the Set is given in parentheses. n.d., no signal detected.

[c] Presence of transcript according to Sreenivasulu et al. (2008). P, pericarp; E, endosperm; U, unspecific; n.d., no signal detected.

[d] Amplitude of the diurnal fluctuation of gene expression given as the ratio of the median normalized maximum signal intensity to the median normalized minimum signal intensity.

Supplemental data files

Figure S1. Quantitative real time PCR (qPCR) of selected genes. Transcript levels were normalized to three reference genes. The resulting expression profiles were compared to those obtained from the microarray experiments. The signal intensities are normalized to the mean expression values and are plotted in log-scale. The respective genes are a putative Gigantea ortholog (*GI-like*), the WRKY transcription factor genes *HvWRKY41* and *HvWRKY46*, the sucrose: fructan-6-fructosyltransferase gene (*Hv6-SFT*), the limit dextrinase gene (*HvLD*), a cyclophilin gene (*HvCycl*), a putative ortholog for the salt tolerance gene (*STO-like*) and the beta-amylase 5 gene (*HvBAM5*).

Figure S2. Principle Component Analysis of the dataset. The global trajectories of the first six principle components are shown as PC1 to PC6 in the diurnal cycle with the six different time points indicated in the x-axis. The contribution of each PC-trajectory to the entire experiment's variance is given in percent.

Figure S3. Gene Ontology classification of genes belonging to six k-means clusters according to GO groups Cellular Component and Molecular Function. The percentage of genes contained in a particular GO group is shown for all present probesets detected by the microarray (17,416 expressed), all DE genes (2,091 genes) and the subsets of genes belonging to clusters 1 to 6 (Set1 to Set 6). Asterisks indicate a significant over- or underrepresentation of functional categories compared to the functional categories of all expressed genes with putative orthologs in Arabidopsis (* $p \leq 0.01$; ** $p \leq 0.001$; *** $p \leq 0.0001$).

Figure S4. GO classification of genes with expression profiles that correlate and anti-correlate to sucrose contents. GO classifications Biological Process, Cellular Component and Molecular Function are shown. The percentage of genes contained in a particular GO group is shown for all present probesets detected by the microarray (grey bars) in comparison to all positively correlated genes (blue bars, correlation factor >0.8) and negatively correlated genes (red bars, correlation factor <-0.8). Asterisks indicate a

significant over- or underrepresentation of functional categories compared to the functional categories of 17,416 expressed genes (* $p \leq 0.01$; ** $p \leq 0.001$; *** $p \leq 0.0001$).

Table S1. Normalized signal intensities and maximum amplitudes of 17,416 present probesets on the Barley1 GeneChip microarray. HarvEST annotations for best BLAST matches in UniProt, rice and Arabidopsis are shown.

Table S2. List of 2,091 DE genes. HarvEST annotations for best BLAST matches in UniProt, rice and Arabidopsis are shown.

Table S3. List of genes sorted to Sets 1 to 6. HarvEST annotations for best BLAST matches in UniProt, rice and Arabidopsis are shown.

Table S4. Overlap of principal components and k-means clusters. List of genes of clusters Set 1 to Set 6 with a correlation positive or negative correlation coefficient of at least 0.8 or 0.9 to PC 1 to PC3. HarvEST annotations for best BLAST matches in UniProt, rice and Arabidopsis are shown.

Table S5. Results of an uncorrected Wilcoxon Rank test performed in MapMan. A selection of sub-groups that belong to frequently occuring BINs with a p-value bigger than 0.05 are highlighted by different shadings.

Table S6. Contents of sugars and amino acids in caryopses of barley 11 to 12 days post anthesis. Values given are mean values of three replicates and standard deviation.

Table S7. List of genes that were positively or negatively correlated to sugars and amino acids. HarvEST annotations for best BLAST matches in UniProt, rice and Arabidopsis are shown.

Table S8. Presence of transcripts in the different suborgan tissues of the caryopsis. Gene lists are presented for genes expressed specifically in pericarp, endosperm and embryo

tissues; genes diurnally regulated in pericarp, endosperm and embryo tissues; genes lists for specific expression in one of the tissues and in addition diurnal DE. HarvEST annotations for best BLAST matches in UniProt, rice and Arabidopsis are shown.

Table S9. List of primers used for qPCR experiments.

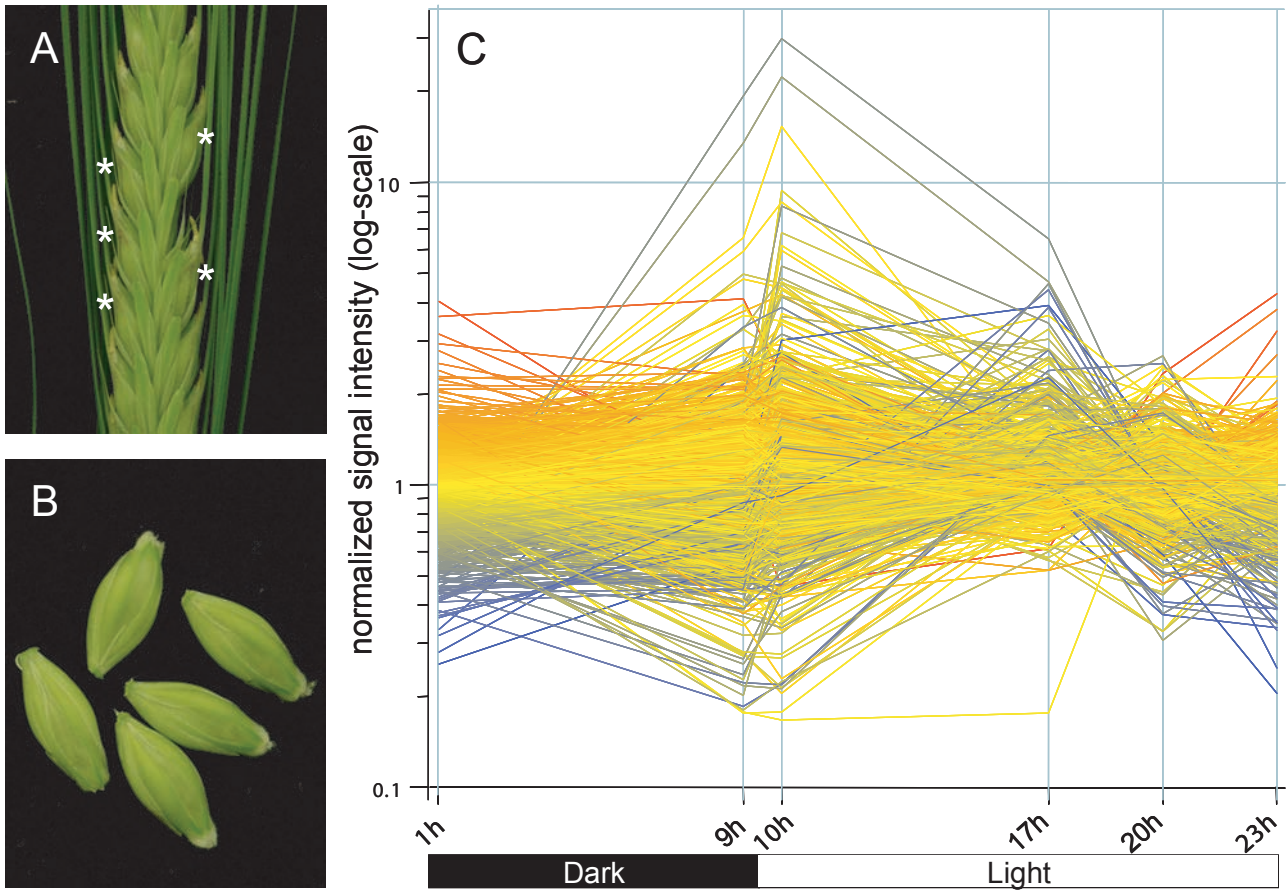

Figure 1. Sampling of plant material and profiles of differentially expressed genes. A, Central region of a barley spike. One floret was removed to determine the onset of flowering. At 12 days post anthesis (d.p.a.) the five barley caryopses closest to the floret used for determination of the onset of anthesis were harvested (white asterisks). B, Prior to pooling and freezing the samples, awns and possibly remaining anthers were removed from the caryopses. C, Expression profile of 2,091 differentially expressed (DE) genes during the diurnal cycle. Six time points of harvest in dark and light phase are indicated at the x-axis as follows: beginning and end of the dark phase (1h and 9h), beginning of the light phase (10h), middle of the light phase (17 and 20h) and end of the light phase (23h).

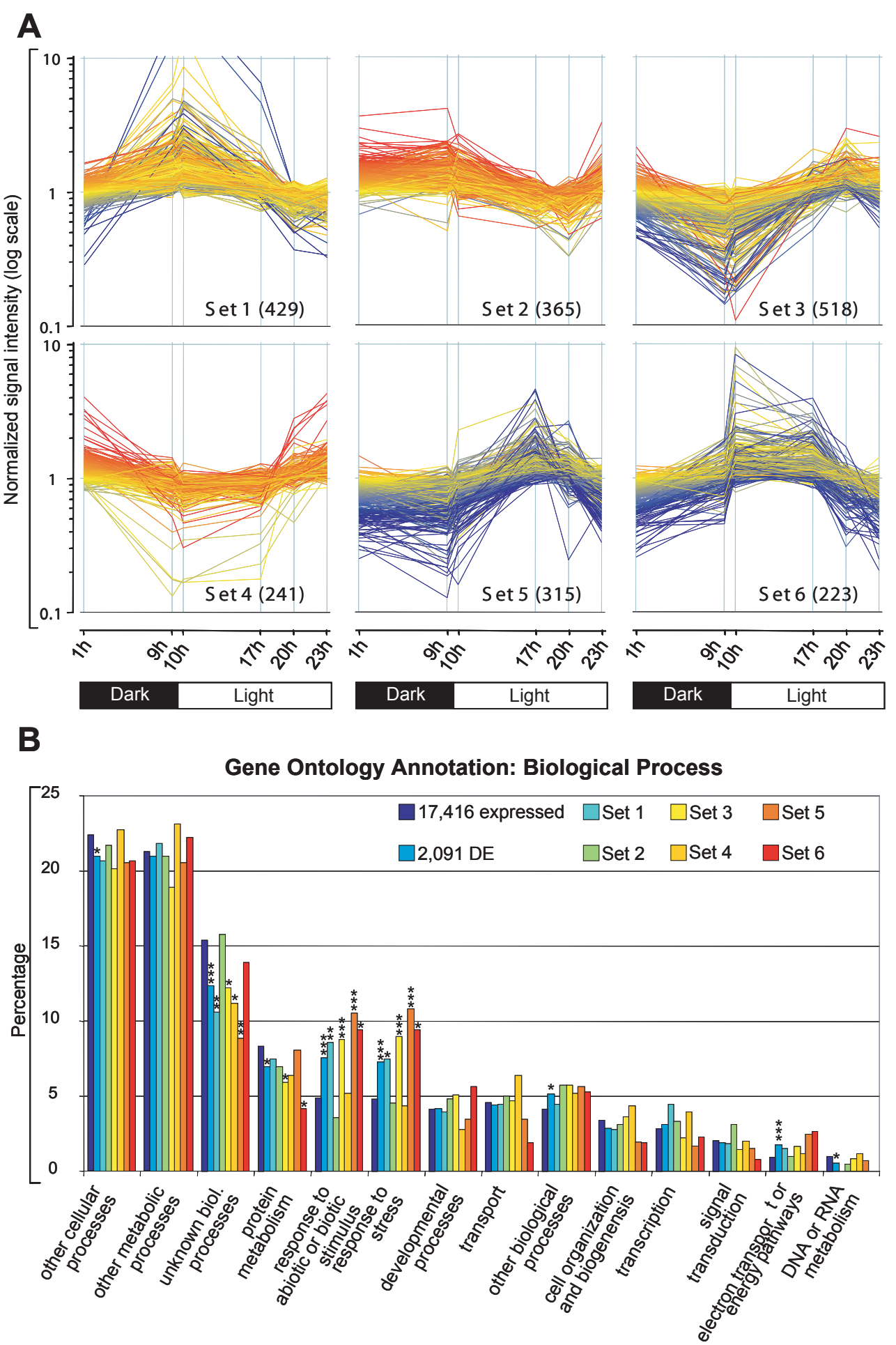

Figure 2. Expression patterns of k-means clusters of DE genes and their classification into functional categories of Gene Ontology (GO). A, Gene expression trajectories of the k-means clusters named Set 1 to 6. The respective six time points are indicated at the x-axis. Total numbers of assigned probesets are given in parentheses. Colors of the profiles depict the normalized transcript level of the probeset at 1h: red, high expression; yellow, moderate expression; blue, low expression. B, Classification of genes according to GO groups for Biological Processes. The number of genes belonging to a particular GO group is shown as percentage for all present probesets detected by the microarray (17,416 expressed), all DE genes (2,091 genes) and the subsets of genes belonging to clusters 1 to 6 (Set 1 to Set 6). Asterisks indicate a significant over- or underrepresentation of functional categories compared to the functional categories of all expressed genes with putative orthologs in Arabidopsis (* $p \leq 0.01$; ** $p \leq 0.001$; *** $p \leq 0.0001$).

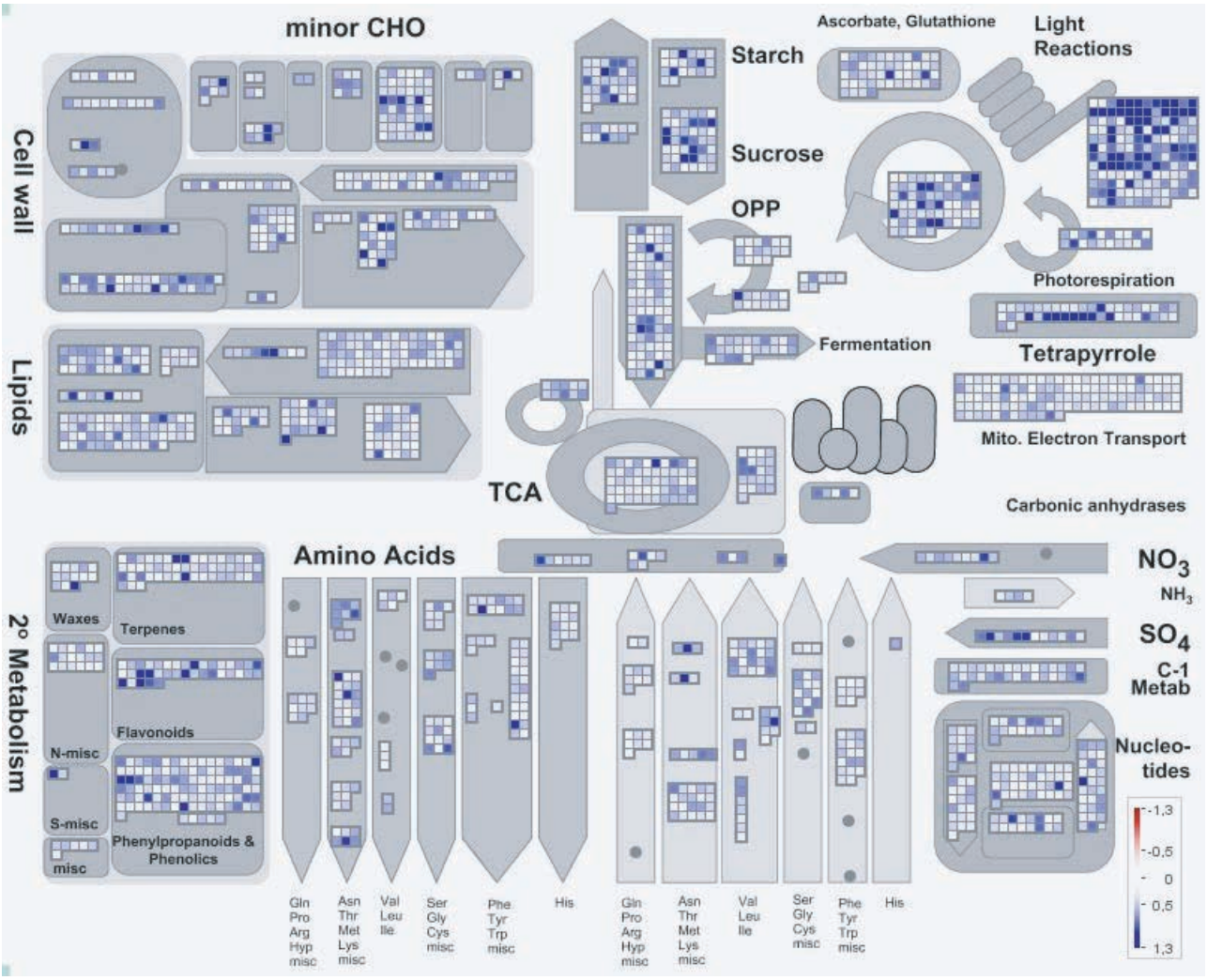

Figure 3. MapMan display showing diurnal amplitudes of 17,416 present genes in a metabolism overview map. Genes on the Barley1 microarray are represented by individual squares. Genes with increasingly large amplitudes are shown as an increasingly intense blue saturating at an amplitude of 1.3 (log2-value). Genes with no significant change in the amplitude are shown in white. Abbreviations used in the Figure: TCA, tricarboxylic acid; CHO, carbohydrate; OPP, oxidative pentose phosphate.

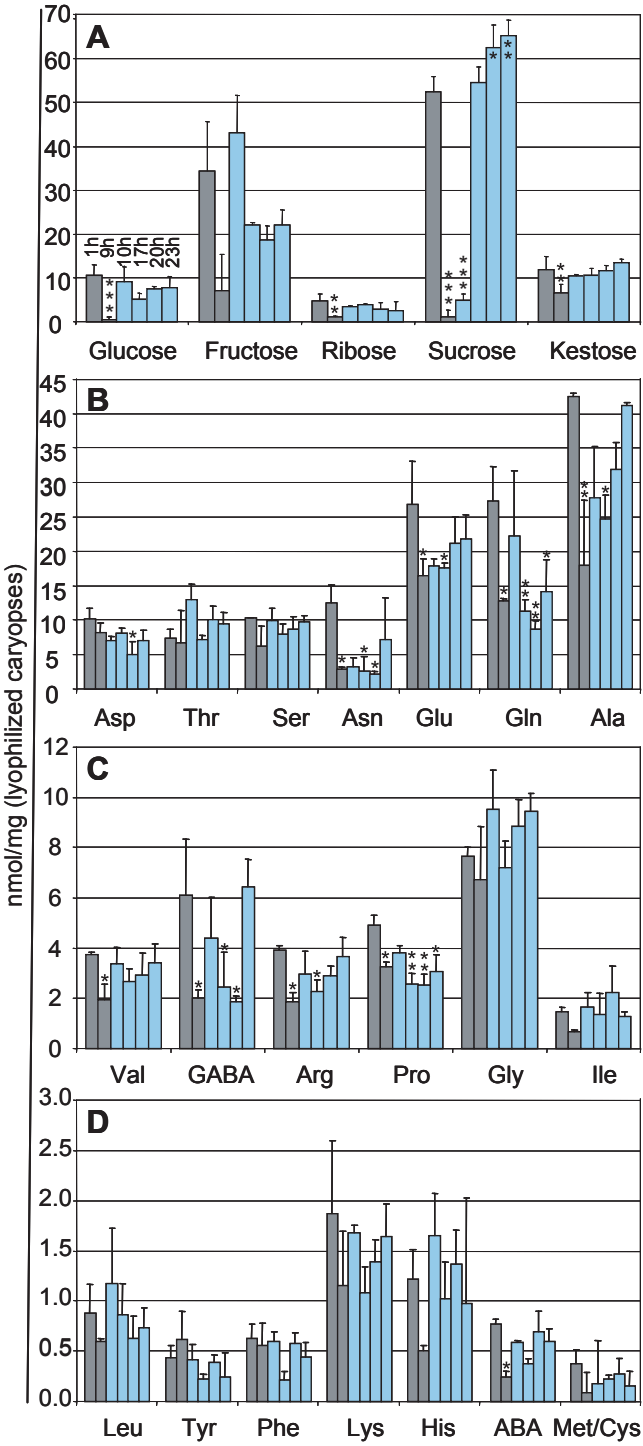

Figure 4. Levels of sugars and amino acids undergo diurnal fluctuations in developing caryopses of barley. A, The amount of sugars was determined at six times during the day. B, C and D, The amount of indicated amino acids was determined at six times during the day. Sampling times were as indicated for the glucose samples in A. Grey and light blue bars depict times in darkness and light, respectively. The data are displayed as mean plus standard deviation. Significant differences compared to the first sample (1h) are indicated by asterisks (*p≤0.01; ** p≤ 0.001; *** p≤0.0001).

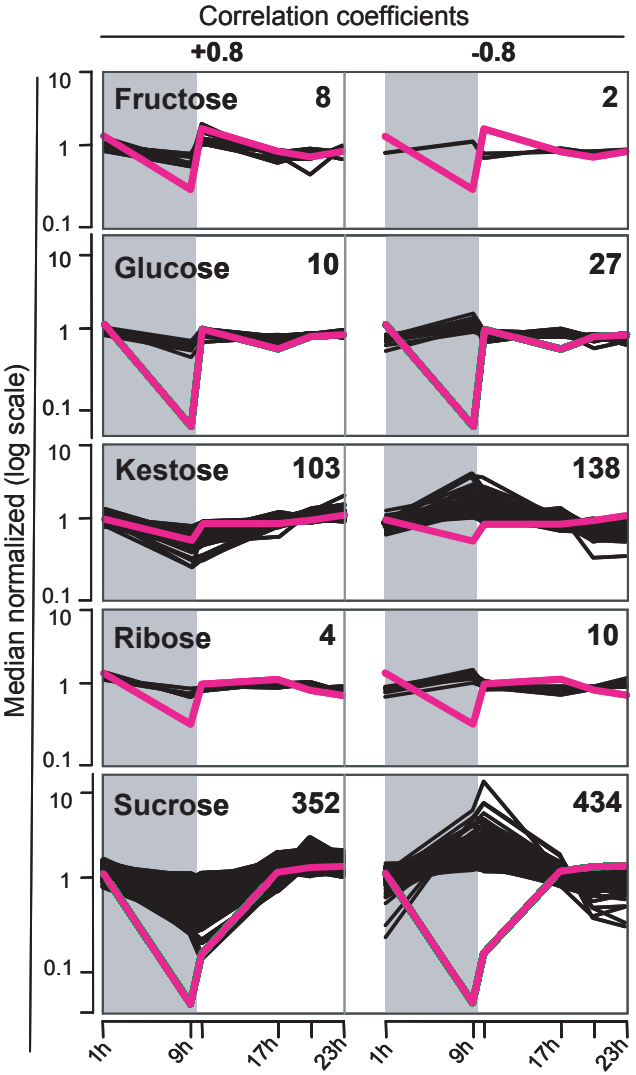

Figure 5. Correlation of sugar contents and expression profiles. Profiles of the indicated sugars and their correlating and anti-correlating gene expression profiles are shown as pink or black lines, respectively. Time points are indicated at the x-axis. Numbers of correlating and anti-correlating genes are displayed for each of the diagrams. Sugar contents and signal intensities are normalized to the mean and plotted in log-scale.

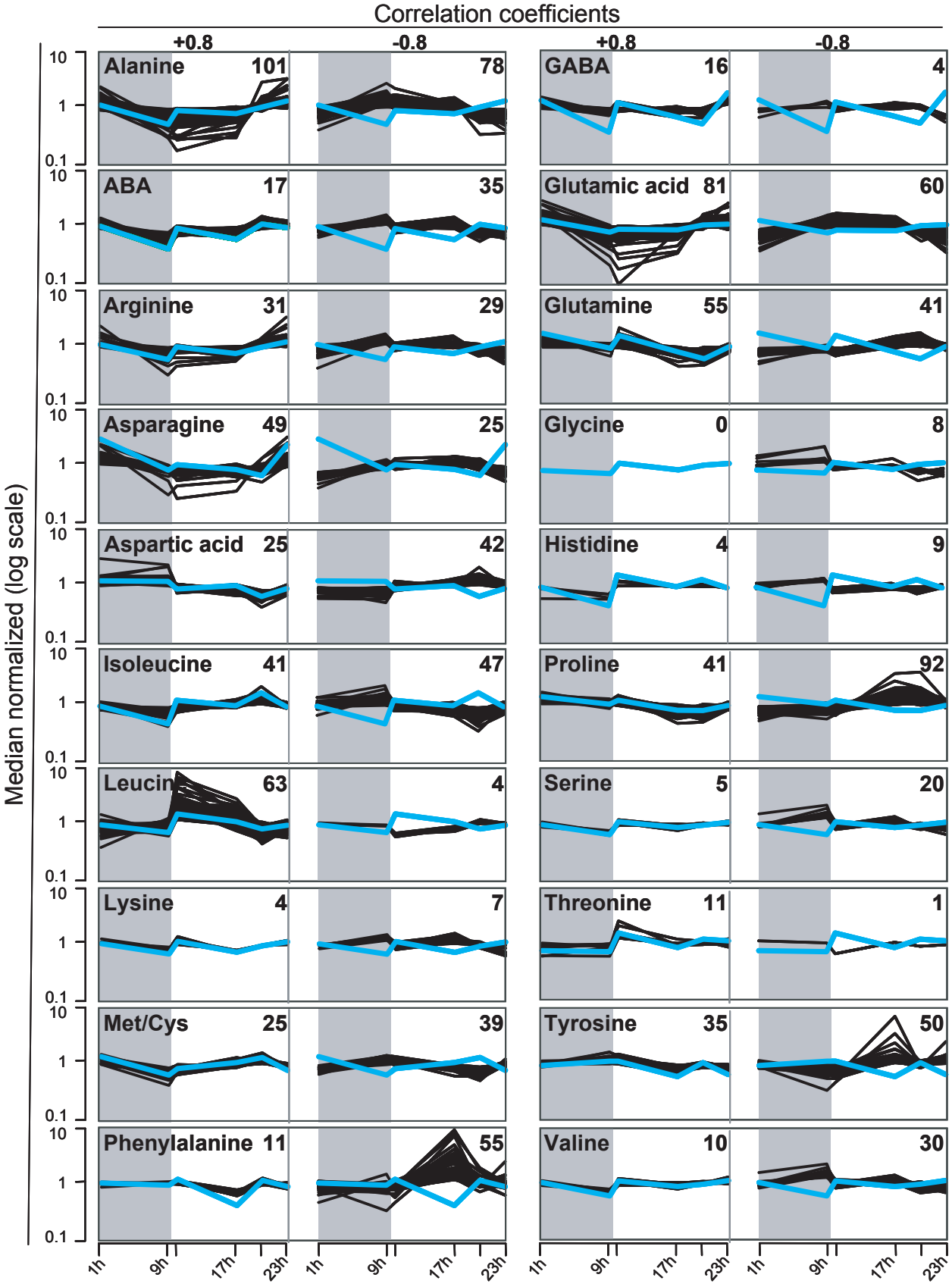

Figure 6. Correlation of amino acid contents and expression profiles. Profiles of the indicated amino acids and their correlating and anti-correlating gene expression profiles are shown as blue or black lines, respectively. Numbers of correlating and anti-correlating genes are displayed for each of the diagrams, time points are indicated at the bottom. The amino acid contents and signal intensities are normalized to the mean and plotted in log-scale.

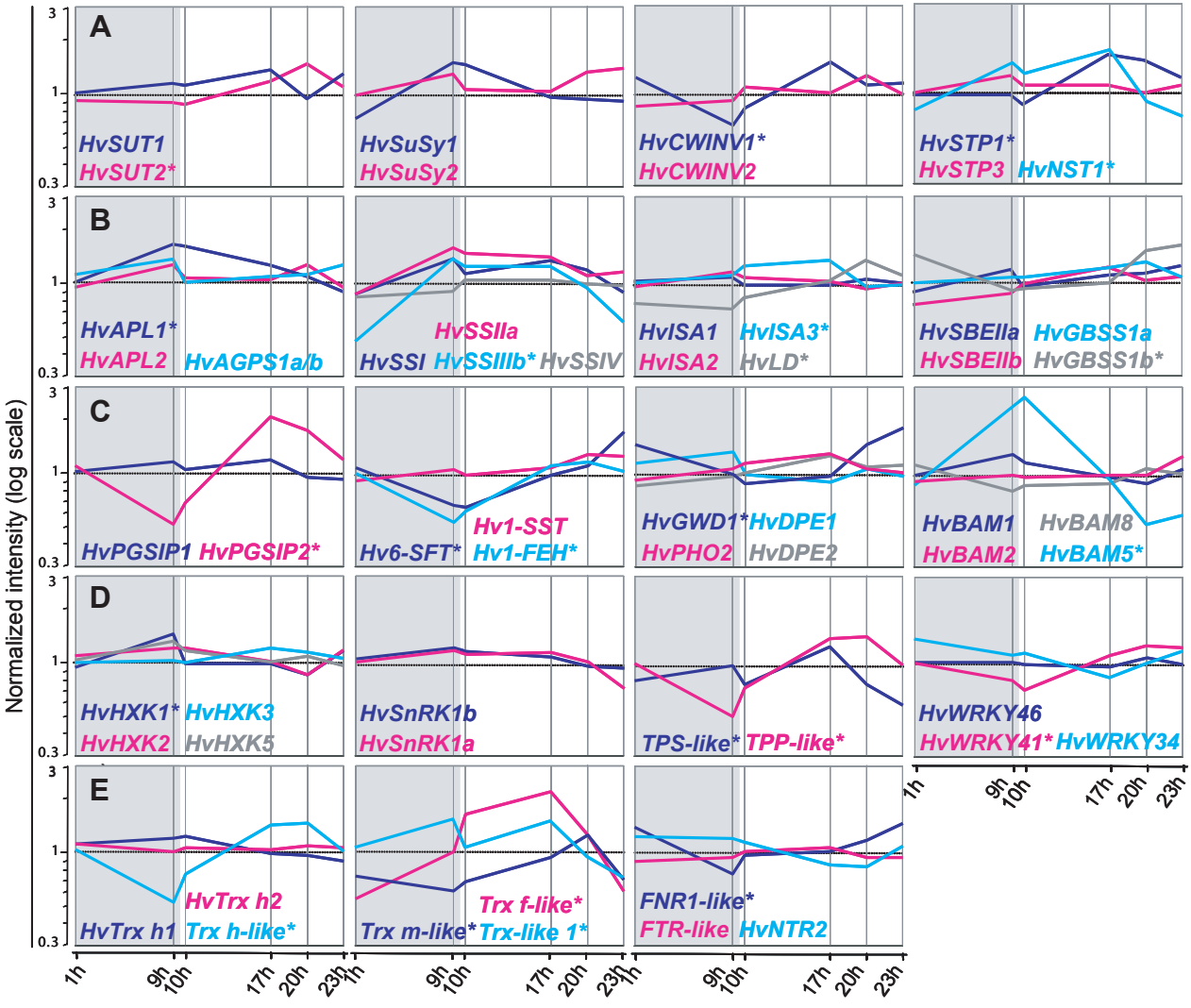

Figure 7. Gene expression profiles of genes involved in sugar metabolism and signaling. Signal intensities at indicated time points during the day are normalized to the mean expression values and plotted in log-scale. Genes are grouped based on their involvement in different pathways as follows: Initial sugar transport and processing (A), starch and fructan synthesis and degradation (B,C), potential sugar signaling (D), ferredoxin/thioredoxin system (E). DE genes are indicated by asterisks. For complete gene names please refer to Table 1.

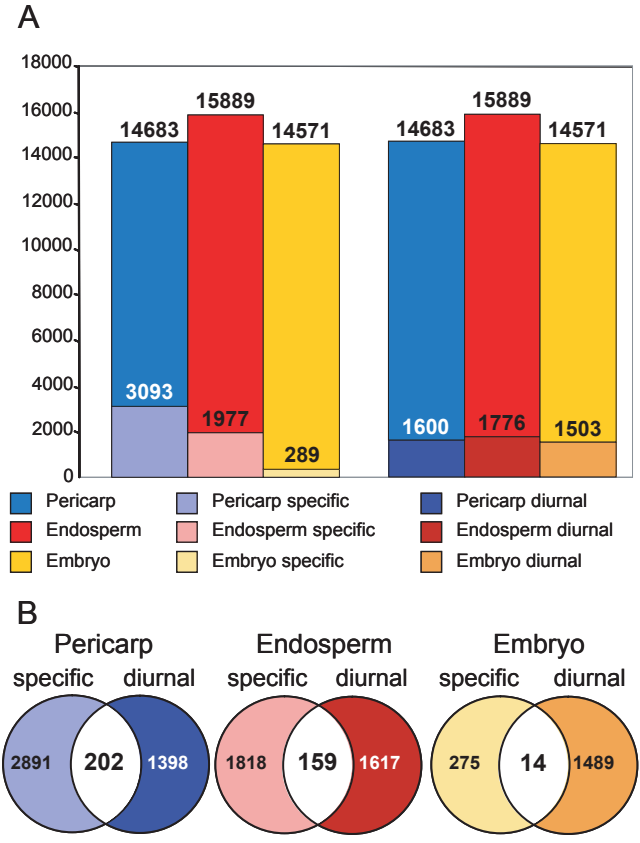

Figure 8. Diurnal gene expression in suborgan tissues of the caryopses. (A) The total number of genes that were expressed in the suborgans pericarp, endosperm and embryo are shown in blue, red and yellow, respectively. Subsets of genes that were exclusively expressed in one suborgan are shown in light-shaded colors. Diurnally expressed genes are depicted in dark-shaded colors. (B) Venn diagrams depicting the exclusive and interference of suborgan-specific and diurnally regulated genes.

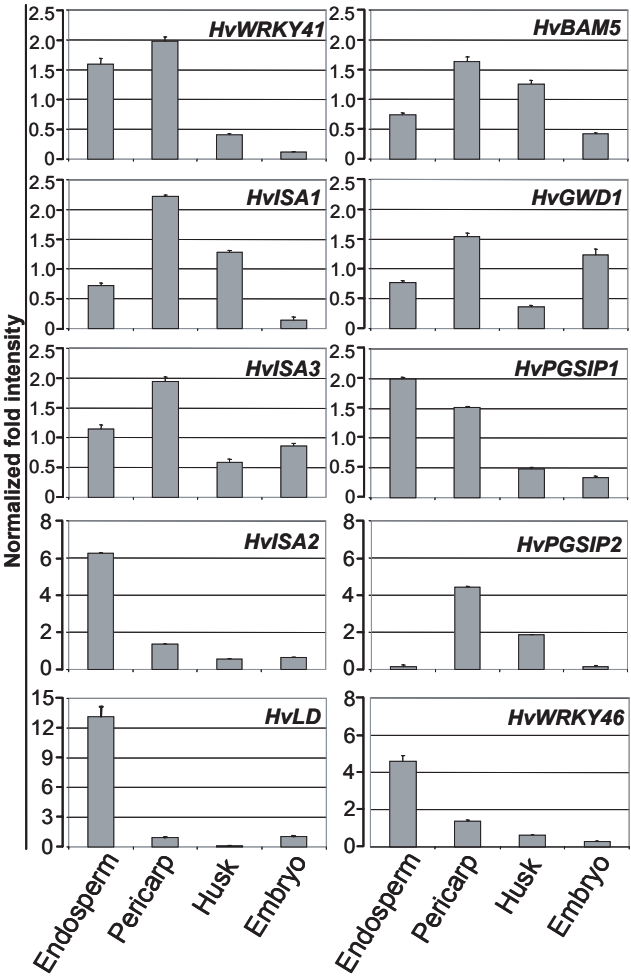

Figure 9. Presence of transcripts in four different tissues of the developing barley caryopsis. Normalized transcript abundance of selected genes were determined by qPCR. Expression levels in endosperm, pericarp, husk and embryo tissues are shown. Results are displayed for genes coding for the following proteins: WRKY transcription factor 41 (HvWRKY41), beta-Amylase 5 (HvBAM5), Isoamylase 1 (HvISA1), Glucan Water Dikinase 1 (HvGWD1), Isoamylase 3 (HvISA3), Plant Glycogenin-like Starch Initiation Protein 1 (HvPGSIP1), Isoamylase 2 (HvISA2), Plant Glycogenin-like Starch Initiation Protein 2 (HvPGSIP2), Limit Dextrinase (HvLD) and WRKY transcription factor SUSIBA2 (HvWRKY46).

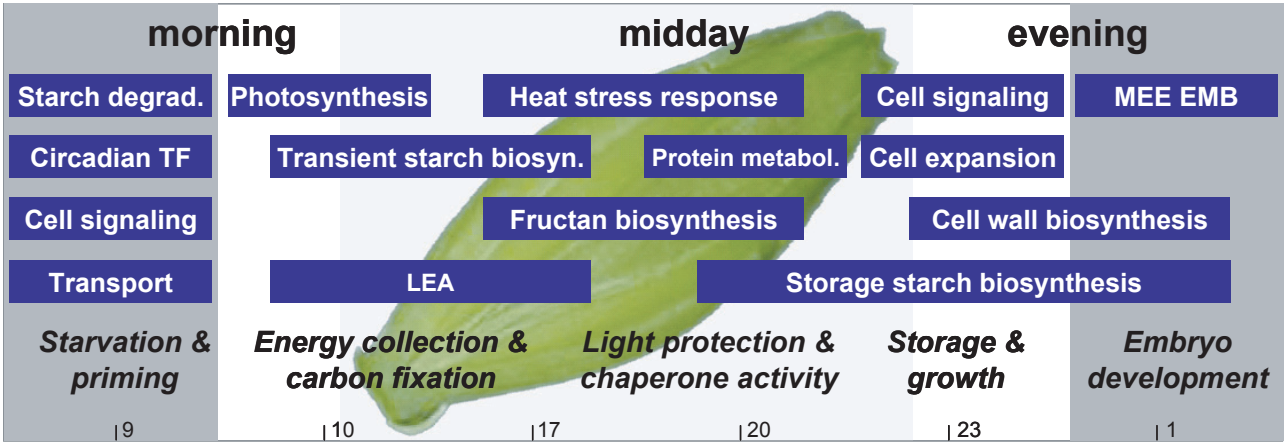

Figure 10. Schematic overview of the diurnal expressional trends in developing caryopses of barley. Functional groups of DE genes with high transcript levels at the investigated times of the day, summarized as morning, midday and evening, are depicted as blue boxes. The length of the blue boxes is indicative for the duration of high expression levels over just one or several investigated time points that are indicated at the bottom of the model. Five phases of diurnal adaptation, named starvation & priming, energy collection & carbon fixation, light protection & chaperone activity, storage & growth, and embryo development, were defined and are indicated in italics. White and grey areas depict light and dark phases of the day, respectively. TF, Transcription factors; LEA, Late embryo abundant proteins; EMB, Embryo defective proteins.

DISCLAIMER

This document was prepared as an account of work sponsored by the United States Government. While this document is believed to contain correct information, neither the United States Government nor any agency thereof, nor the Regents of the University of California, nor any of their employees, makes any warranty, express or implied, or assumes any legal responsibility for the accuracy, completeness, or usefulness of any information, apparatus, product, or process disclosed, or represents that its use would not infringe privately owned rights. Reference herein to any specific commercial product, process, or service by its trade name, trademark, manufacturer, or otherwise, does not necessarily constitute or imply its endorsement, recommendation, or favoring by the United States Government or any agency thereof, or the Regents of the University of California. The views and opinions of authors expressed herein do not necessarily state or reflect those of the United States Government or any agency thereof or the Regents of the University of California.